

Manuscript Number: SAMES-D-15-00118

Title: The Archean-Paleoproterozoic evolution of the Quadrilátero Ferrífero (Brasil): current models and open questions

Article Type: SI: Granite magmatism

Keywords: Quadrilátero Ferrífero; Archean; Paleoproterozoic; tectonomagmatic evolution

Abstract: The Quadrilátero Ferrífero is a metallogenic district (Au, Fe, Mn) located at the southernmost end of the São Francisco craton in eastern Brazil. In this region, a supracrustal assemblage composed of Archean greenstone and overlying Neoproterozoic sedimentary rocks occur in elongated keels bordering domal bodies of Archean gneisses and granites. The tectonomagmatic evolution of the Quadrilátero Ferrífero began in the Paleoproterozoic with the formation of continental crust between 3500 and 3200 Ma. Although this crust is today poorly preserved, its existence is attested to by the occurrence of detrital zircons in the supracrustal rocks. Most of the Quadrilátero crystalline basement, which is composed of banded gneisses intruded by leucogranitic dikes and weakly foliated granites, formed during three major magmatic events: Rio das Velhas I (2920-2850 Ma), Rio das Velhas II (2800-2760 Ma) and Mamona (2760-2680 Ma). The Rio das Velhas II and Mamona events represent a subduction-collision cycle, likely marking the action of a modern-style plate tectonic regime in the Quadrilátero Ferrífero region. Granitic rocks emplaced during the Rio das Velhas I and II events formed by mixing between a magma generated by partial melting of metamafic rocks with an end member derived by recycling gneissic rocks of older continental crust. After deformation and regional metamorphism at ca. 2770 Ma, a change in the composition of the granitic magmas occurred and large volumes of high-K granitoids were generated.

The ca. 6000 m-thick Minas Supergroup tracks the operation of a Wilson cycle in the Paleoproterozoic between 2600 and 2000 Ma. The basal sequence involves continental to marine sediments deposited in a passive margin basin and contain as a marker bed the Lake Superior-type Cauê Banded Iron Formation. The overlying sediments of the Sabará Group mark the inversion of the basin during the Rhyacian Minas accretionary orogeny. This orogeny, resulting from the collision between the nuclei of the present-day São Francisco and Congo cratons, generated the fold-and thrust belt structure of the Quadrilátero Ferrífero. Afterwards, the post-collisional orogenic collapse resulted in the deposition of the Itacolomi Group and in the genesis of the dome-and-keel structure.

In this paper, we review current knowledge about the 1500 Ma long-lasting tectonomagmatic and structural evolution of the Quadrilátero Ferrífero identifying the most compelling open questions and future challenges.

1  
2  
3  
4  
5  
6  
7  
8  
9  
10  
11  
12  
13  
14  
15  
16  
17  
18  
19  
20  
21  
22  
23  
24  
25  
26  
27  
28  
29  
30  
31  
32  
33  
34  
35  
36  
37  
38  
39  
40  
41  
42  
43  
44  
45  
46  
47  
48  
49  
50  
51  
52  
53  
54  
55  
56  
57  
58  
59  
60  
61  
62  
63  
64  
65

1 **The Archean-Paleoproterozoic evolution of the Quadrilátero Ferrífero (Brasil): current**  
2 **models and open questions**

3  
4  
5  
6  
7  
8  
9  
10  
11  
12  
13  
14  
15  
16  
17  
18  
19  
20  
21  
22  
23  
24  
25  
26  
27  
28  
29  
30  
31  
32  
33  
34  
35  
36  
37  
38  
39  
40  
41  
42  
43  
44  
45  
46  
47  
48  
49  
50  
51  
52  
53  
54  
55  
56  
57  
58  
59  
60  
61  
62  
63  
64  
65

4 Farina, F., Albert, C., Martinez Dopico, C., Aguilar Gil, C., Moreira, H., Hippertt, J.P., Cutts, K.,  
5 Alkmim, F.F., Lana, C.

8 **Abstract**

9 The Quadrilátero Ferrífero is a metallogenic district (Au, Fe, Mn) located at the southernmost  
10 end of the São Francisco craton in eastern Brazil. In this region, a supracrustal assemblage  
11 composed of Archean greenstone and overlying Neoproterozoic sedimentary  
12 rocks occur in elongated keels bordering domal bodies of Archean gneisses and granites. The  
13 tectonomagmatic evolution of the Quadrilátero Ferrífero began in the Paleoproterozoic with the  
14 formation of continental crust between 3500 and 3200 Ma. Although this crust is today poorly  
15 preserved, its existence is attested to by the occurrence of detrital zircons in the supracrustal  
16 rocks. Most of the Quadrilátero crystalline basement, which is composed of banded gneisses  
17 intruded by leucogranitic dikes and weakly foliated granites, formed during three major  
18 magmatic events: Rio das Velhas I (2920-2850 Ma), Rio das Velhas II (2800-2760 Ma) and  
19 Mamona (2760-2680 Ma). The Rio das Velhas II and Mamona events represent a subduction-  
20 collision cycle, likely marking the action of a modern-style plate tectonic regime in the  
21 Quadrilátero Ferrífero region. Granitic rocks emplaced during the Rio das velhas I and II events  
22 formed by mixing between a magma generated by partial melting of metamafic rocks with an  
23 end member derived by recycling gneissic rocks of older continental crust. After deformation

1  
2  
3  
4  
5  
6  
7  
8  
9  
10  
11  
12  
13  
14  
15  
16  
17  
18  
19  
20  
21  
22  
23  
24 and regional metamorphism at ca. 2770 Ma, a change in the composition of the granitic  
25 magmas occurred and large volumes of high-K granitoids were generated.

26 The ca. 6000 m-thick Minas Supergroup tracks the operation of a Wilson cycle in the  
27 Paleoproterozoic between 2600 and 2000 Ma. The basal sequence involves continental to  
28 marine sediments deposited in a passive margin basin and contain as a marker bed the Lake  
29 Superior-type Cauê Banded Iron Formation. The overlying sediments of the Sabará Group mark  
30 the inversion of the basin during the Rhyacian Minas accretionary orogeny. This orogeny,  
31 resulting from the collision between the nuclei of the present-day São Francisco and Congo  
32 cratons, generated the fold-and thrust belt structure of the Quadrilátero Ferrífero. Afterwards,  
33 the post-collisional orogenic collapse resulted in the deposition of the Itacolomi Group and in  
34 the genesis of the dome-and-keel structure.

27  
28  
29  
30  
31  
32  
33  
34  
35  
36  
37  
38  
39  
40  
41  
42  
43  
44  
45  
46  
47  
48  
49  
50  
51  
52  
53  
54  
55  
56  
57  
58  
59  
60  
61  
62  
63  
64  
65  
In this paper, we review current knowledge about the 1500 Ma long-lasting tectonomagmatic  
and structural evolution of the Quadrilátero Ferrífero identifying the most compelling open  
questions and future challenges.

## 39 **1. Introduction**

40 In the mid-twentieth century, the ca. 7000 km<sup>2</sup> portion of the Brazilian highlands south of the  
41 city of Belo Horizonte (Fig. 1) became well-known under the name of Quadrilátero Ferrífero  
42 (“Iron Quadrangle”). This region, which has been an important mining site since the XVIII  
43 century, represents the most intensively studied region of Brazil. Its valuable iron and gold  
44 deposits together with its puzzling geological complexity have attracted the attention of many  
45 scientists over the last century. The goal of the present paper is to provide an up-to-date state  
46 of the art on the geology of the Archean crystalline basement and Archean-Paleoproterozoic  
47 metasedimentary sequences forming the Quadrilátero Ferrífero. This review, focussed on the  
48 Archean and Paleoproterozoic evolution of this portion of the southern São Francisco craton, is

1  
2  
3  
4  
5  
6  
7  
8  
9  
10  
11  
12  
13  
14  
15  
16  
17  
18  
19  
20  
21  
22  
23  
24  
25  
26  
27  
28  
29  
30  
31  
32  
33  
34  
35  
36  
37  
38  
39  
40  
41  
42  
43  
44  
45  
46  
47  
48  
49 not aiming to be exhaustive. Some important topics will not be addressed (e.g. the origin of  
50 ore deposits) while others will be only briefly presented (e.g. the structural evolution). The  
51 goal of this contribution is to discuss the present-day petrologic and geodynamic models  
52 proposed for the Quadrilátero, drawing attention to the main open problems and limitations in  
53 an attempt to highlight future challenges and favourable research directions.

54

## 55 **2. Historical background and geographic boundaries**

56 In the sixteenth century, the discovery of large gold and silver deposits in the Spanish colonial  
57 possessions in South America (e.g. the Potosí silver deposits in Bolivia) triggered the  
58 Portuguese empire to embark in the exploration of inland Brazil seeking precious metals. From  
59 1545, the Portuguese colonial government organized and financed many expeditions as well as  
60 encouraging private expeditions (i.e. the “bandeiras”) that were mostly organized by  
61 adventurers from the São Paulo region (the Captaincy of São Vicente). For ca. 100 years the  
62 hunt for payable precious metals proved futile and only in 1646 the first discovery of small  
63 alluvial gold deposit in Brazil was made in the southern state of Paraná (Figueiredo, 2011; Fig.  
64 2). In 1693, the first gold placer deposit was found in southeastern Brazil (state of Minas  
65 Gerais), close to the city of Ouro Preto (“black gold” in Portuguese). The discovery of many rich  
66 gold deposits in the region that is today known as the Quadrilátero Ferrífero, revitalized  
67 Brazil’s economy, which had been stagnating since the decline of the sugar plantations (Costa  
68 et al., 2003). Gold discovery caused such a stir that, by the end of the century a considerable  
69 proportion of Sao Paulo’s, Rio de Janeiro’s and the northern province of Bahia’s population  
70 had rushed to the site of the discovery. More significantly, as news of the discovery spread to  
71 the mother country, thousands of Portuguese adventurers moved to Brazil at the turn of the  
72 eighteenth century: the first great gold rush had begun. Between 1693 and 1720, the  
73 population of the gold-rich province grew exponentially; i.e. in that period, about 400000

60  
61  
62  
63  
64  
65

1  
2  
3  
4  
5  
6  
7  
8  
9  
10  
11  
12  
13  
14  
15  
16  
17  
18  
19  
20  
21  
22  
23  
24  
25  
26  
27  
28  
29  
30  
31  
32  
33  
34  
35  
36  
37  
38  
39  
40  
41  
42  
43  
44  
45  
46  
47  
48  
49  
50  
51  
52  
53  
54  
55  
56  
57  
58  
59  
60  
61  
62  
63  
64  
65

74 Portuguese and 500000 slaves had relocated to southeastern Brazil to mine gold. Such was the  
75 growth that half Brazil's entire population was residing in Minas Gerais in 1725. Gold  
76 production increased as the eighteenth century advanced, peaking around mid-century and  
77 then, due to the rudimental mining technique implemented (e.g. mostly panning and sluicing  
78 in shallow water stream) slowly declined but continuing into the nineteenth century (Costa et  
79 al., 2003).

80 By the beginning of the nineteenth century, many European explorers and naturalists carried  
81 out geographic and geological studies in the gold-bearing province (Fig.2; Machado, 2009). In  
82 1810, the mineralogist and geologist Baron Wilhelm Ludwig von Eschwege arrived to Brazil  
83 entrusted by the king Dom João VI to study the ores and the mining activity with the goal of  
84 implementing new mining techniques to increase gold production. The baron, defined by  
85 Derby (1906), "the founder of Brazilian Geology" made a significant step forward in the  
86 description and understanding of the geology of the Quadrilátero Ferrífero. Eschwege  
87 published various books (e.g. *Jornal do Brasil, 1811-1817; Pluto brasiliensis (1833)*) in which he  
88 outlined the main geological features of the Precambrian terranes of central Brazil proposing a  
89 stratigraphic subdivision according to Werner's Neptunism theory. Moreover, the baron also  
90 produced the first cross-section from Rio de Janeiro to Vila Rica (the old name of Ouro Preto).  
91 The work of Eschwege was influential and guided many other foreign naturalists that visited  
92 Brazil in the eighteenth century such as Peter Claussen (1805-1852), Aimé Pissis (1812-1889)  
93 and the geologist and mining engineer Virgil von Helmreichen (1802-1855) who produced the  
94 first geological maps of the region surrounding the city of Ouro Preto (Machado, 2009).

95 In the early twentieth century, the gold-rich region around Ouro Preto returned to the  
96 spotlight because of its iron and manganese deposits. One century after Eschwege arrived in  
97 Brazil, the American geologist Derby published a work titled "The iron ores of Brazil" that  
98 attracted the interest of the mining community to the iron and manganese deposits of Minas

99 Gerais. In the mid-twentieth century, an agreement was set between the Brazilian National  
100 Department of Mineral Production (DNPM) and the U.S. Geological Survey to undergo the first  
101 detailed geological study of the region where the main iron and manganese deposits were  
102 located (Machado, 2009). This agreement and the two decades of work that followed marked  
103 the most important step forward in the understanding of the geology of the Quadrilátero  
104 Ferrífero. The outcome of this joint project was a set of 42 geological maps in the 1:25.000  
105 scale followed by a stratigraphic column and a report written by the head of the team, John  
106 Van N. Dorr II, in which the main geological features of the studied region were defined. Dorr  
107 and collaborators used the term Quadrilátero Ferrífero in 1952 (Machado, 2009) to give credit  
108 to the abundance of high-grade iron ore deposits in the region. These authors defined the  
109 geographic boundaries of the Quadrilátero producing a detailed 1:150.000 geological map.  
110 Oddly, as shown in figure 1, the “iron quadrangle” of Dorr and collaborators is not a  
111 quadrangle but rather a complex polygon, including the Itabira mining district. The reason for  
112 the use of the term Quadrilátero proposed by Dorr is historical. In fact, the term was  
113 introduced in 1923 by the Brazilian geologist Luis Flores de Moraes Rego in a paper titled “As  
114 jazidas de ferro do centro de Minas Gerais” (i.e. “The iron ores of central Minas Gerais”) to  
115 define the four-sided area comprised between the cities of Belo Horizonte, Santa Bárbara,  
116 Congonhas and Mariana (Machado, 2009). Clear geographic features do not delimit the  
117 Quadrilátero Ferrífero as defined and mapped by Dorr and collaborators and thus, the term  
118 has been used loosely to describe the geology of areas that are not part of the original map of  
119 the Quadrilátero. As shown in Figure 1, we will also extend the limits of the Quadrilátero  
120 Ferrífero to include the Bonfim and the Belo Horizonte domes in their entirety.

121

### 122 **3. Main geological features**

1  
2  
3  
4  
5  
6  
7  
8  
9  
10  
11  
12  
13  
14  
15  
16  
17  
18  
19  
20  
21  
22  
23  
24  
25  
26  
27  
28  
29  
30  
31  
32  
33  
34  
35  
36  
37  
38  
39  
40  
41  
42  
43  
44  
45  
46  
47  
48  
49  
50  
51  
52  
53  
54  
55  
56  
57  
58  
59  
60  
61  
62  
63  
64  
65

123 The São Francisco craton in eastern Brazil is one of the major and probably the best-exposed  
124 shield area forming the South American platform. The craton is subdivided into four Archaean  
125 blocks bounded by major ca. 2100 Ma old sutures zones (Teixeira and Figueiredo, 1991;  
126 Barbosa and Sabaté, 2004) and surrounded by Neoproterozoic orogenic belts (e.g. the Araçuaí  
127 and Brasília belts; Pedrosa-Soares, 2001; Pimentel et al., 2011). The northern part of the craton  
128 comprises four crustal segments intensively affected by the Rhyacian-Orosirian orogenic event  
129 (Barbosa and Sabaté, 2004): the Gavião, Jequié, Serrinha and Itabuna-Salvador-Curaçá blocks  
130 (Fig. 1). The basement of the southern São Francisco craton, probably representing an  
131 extension of the Gavião block (Alkmim and Noce, 2006; Lana et al., 2013) comprises various  
132 granitoid-gneiss complexes (i.e. Campo Belo, Passa Tempo, Bonfim, Belo Horizonte, Baçãõ,  
133 Caeté) partially covered by Archean and Paleoproterozoic supracrustal sequences. The  
134 Quadrilátero Ferrífero mining district, occupying the eastern part of the Southern São  
135 Francisco Craton, is fringed by the Ediacaran-Cambrian Araçuaí belt (Pedrosa-Soares et al.,  
136 2001) to the east and by the Paleoproterozoic Mineiro Belt (Teixeira and Figueiredo, 1991) to  
137 the south (Fig. 1). The district exhibits NNW-verging folds and thrusts and has a metamorphic  
138 overprint at about 2100-2000 Ma, which was originally known as the “Minas diastrophism”  
139 (e.g., Cordani et al., 1980). The distinctive structural architecture of the Quadrilátero is its  
140 dome-and keel geometry, in which belts of low-grade Paleoproterozoic supracrustal rocks  
141 surround medium to high-grade granitoid-gneiss Archean complexes (Marshak et al., 1997).  
142 The Quadrilátero Ferrífero can be subdivided into four Archean to Paleoproterozoic  
143 lithostratigraphic units:

- 144 (i) Archean metamorphic complexes composed of gneisses, migmatites, and
- 145 granitoids;
- 146 (ii) the Archean Rio das Velhas Supergroup, formed by greenstone and low- to
- 147 medium-grade metasedimentary units;

- 1  
2  
3  
4  
5  
6  
7  
8  
9  
10  
11  
12  
13  
14  
15  
16  
17  
18  
19  
20  
21  
22  
23  
24  
25  
26  
27  
28  
29  
30  
31  
32  
33  
34  
35  
36  
37  
38  
39  
40  
41  
42  
43  
44  
45  
46  
47  
48  
49  
50  
51  
52  
53  
54  
55  
56  
57  
58  
59  
60  
61  
62  
63  
64  
65
- 148 (iii) the Paleoproterozoic Minas Supergroup, consisting of low- to medium-grade  
149 metasedimentary rocks;  
150 (iv) the Paleoproterozoic Itacolomi Group composed of metasandstones and  
151 conglomerates.

152 In addition, the Quadrilátero Ferrífero includes small granite bodies and pegmatite veins  
153 locally cutting the youngest strata of the Minas Supergroup as well as different generations of  
154 mafic dikes showing contrasting metamorphic grade, composition and trending direction. A  
155 stratigraphic section of the Quadrilátero Ferrífero is presented in Figure 3 and the different  
156 lithostratigraphic units are described in the following sections.

157

#### 158 4. The Archean metamorphic complexes

159

##### 160 4.1. Field relationships and petrography

161 In the field, the rocks of the basement can be subdivided into three main groups:

- 162 i) fine-grained banded orthogneisses intruded by (ii) and (iii)  
163 ii) leucogranites and aplitic/pegmatitic veins and dikes;  
164 iii) medium- to coarse-grained, mostly weakly foliated granites (*sensu lato*).

165

166 The gneisses are characterised by the alternation between leucocratic and mesocratic, or more  
167 rarely, melanocratic bands, varying in width from 2 mm to up to 10 cm defining a penetrative  
168 amphibolite-facies foliation (Fig. 4). The mesocratic bands are rich in plagioclase and biotite  
169 and display lepidonematoblastic textures, whereas the leucocratic ones, containing  
170 predominantly plagioclase, quartz and minor microcline, show granoblastic textures (Lana et  
171 al., 2013). Alkali-feldspars are generally interstitial, but occasionally form cm-scale  
172 phenocrysts. Locally, the gneisses exhibit a variety of migmatitic structures (Farina et al.,



173 2015). The gneisses are intruded by multiple, meter- to cm-scale leucogranitic sheets sub-  
174 parallel to the gneissosity as well as by crosscutting younger felsic and/or pegmatitic dikes  
175 (Lana et al., 2013). Felsic bodies oriented sub-parallel to the banding (i.e. leucogranitic sheets)  
176 have width ranging from few centimetres to ca. 60 cm and may be either foliated or massive. A  
177 younger generation of leucogranitic, pegmatitic and aplitic dikes that crosscut both the  
178 gneissic banding and the leucogranitic sheets have widths reaching a maximum of about 2  
179 meters. These dikes are only occasionally slightly folded or boudinaged, but in general appear  
180 little stretched, nor shortened.

181 Granitic rocks form texturally and compositionally composite batholiths (e.g. the Mamona  
182 batholith, Fig. 1) as well as relatively small-scale domains and stocks intruded in or closely  
183 associated with the banded gneisses (Farina et al., 2015). Although typically weakly foliated,  
184 granitoids may also locally develop prolate L>S fabric. The granitic rocks are medium- to  
185 coarse-grained and exhibit either equigranular or porphyritic textures ranging in composition  
186 from tonalite to syenogranite. Based on the ferromagnesian minerals contained, three rock  
187 types are recognised: biotite-bearing granodiorites and granites, two-mica granites and biotite-  
188 and amphibole-bearing tonalites and granodiorites. The first group represents the most  
189 abundant granite-type while muscovite- and amphibole-bearing granitoids are rare, mostly  
190 cropping out in the Bonfim complex. The relationship between banded gneisses and granitoids  
191 is observable in some key outcrops in the Baçao and Bonfim complexes. The intrusion of  
192 granites into banded gneisses produces different features. From gneiss- to granite-dominated  
193 outcrops, we observe: i) dikes of medium-grained granites cutting both the gneissic banding  
194 and the leucogranite sheets; ii) complex intermingled gneiss-granite structures; iii) meter- to  
195 decametre-scale domains of granites intruding the banded gneisses; iv) xenoliths of banded  
196 gneisses hosted within granites (Fig. 4).

197

#### 198 *4.2. Geochemistry: medium- and high-K granitoids*

199 Whole rock major and trace element data for granites and gneisses in the Quadrilátero  
1  
2 Ferrífero is scarce, with different contributions generally investigating the compositional  
3  
4  
5 201 variability of individual complexes without attempting any regional-scale correlation (Carneiro  
6  
7 202 et al., 1992; Noce et al., 1997). An exception to this approach is represented by the work of  
8  
9 203 Farina et al. (2015) in which a large database of chemical compositions for the granites and  
10  
11 204 gneisses of the Bação, Bonfim and Belo Horizonte complexes was produced. In figures 5, 6 and  
12  
13  
14 205 7, we plotted the major and trace element composition of gneisses and granitoids from the  
15  
16 206 Bação, Bonfim, Belo Horizonte and Caeté complexes as well as the composition of dacites from  
17  
18 207 the Rio das Velhas greenstone belt. A complete dataset of whole rock compositions is  
19  
20  
21 208 presented in the **Electronic supplement (Table A)**.  
22  
23 209 Gneisses, granitoids and leucogranites of the Quadrilátero Ferrífero are silica-rich (i.e. ca. 70%  
24  
25 210 of samples have silica content higher than 72 wt.%) and all major element oxides are broadly  
26  
27 211 negatively correlated with SiO<sub>2</sub> (Fig. 6), except K<sub>2</sub>O that displays positive correlation.  
28  
29 212 In the normative feldspar classification diagram for granitoids (An–Ab–Or, O’Connor, 1965),  
30  
31 213 most of the gneisses and granites plot either in the trondhjemite or in the granite fields (Fig.  
32  
33 214 5), with only the biotite- and hornblende-bearing Samambaia pluton described by Carneiro  
34  
35 215 (1992) plotting in the field of **tonalities**. The An–Ab–Or diagram reflects the existence of two  
36  
37 216 main groups of rocks exhibiting different potassium over sodium contents. The two groups can  
38  
39 217 be distinguished in the K<sub>2</sub>O vs. SiO<sub>2</sub> diagram where most of the trondjemites of figure 5 plot in  
40  
41 218 the medium-K field defined by Gill (1981) while granitic rocks plot in the high-K field (Fig. 6).  
42  
43 219 The occurrence of medium- and high-K gneisses and granitic rocks in the basement of the  
44  
45 220 Quadrilátero Ferrífero is evident when the K<sub>2</sub>O/Na<sub>2</sub>O of the rocks is plotted in a frequency  
46  
47 221 histogram (Fig. 6). The distribution is bimodal showing well-defined peaks at 0.4-0.6 and 1.2-  
48  
49 222 1.6 K<sub>2</sub>O/Na<sub>2</sub>O. Systematic compositional differences exist between medium- and high-K rocks.  
50  
51 223 Medium-K gneisses and granitoids have higher Al<sub>2</sub>O<sub>3</sub>, Na<sub>2</sub>O, CaO and Sr as well as lower silica  
52  
53 224 and Rb than high-K rocks (Fig. 6). In addition, medium-K granitoids have relatively high  
54  
55  
56  
57  
58  
59  
60  
61  
62  
63  
64  
65

1  
2  
3  
4  
5  
6  
7  
8  
9  
10  
11  
12  
13  
14  
15  
16  
17  
18  
19  
20  
21  
22  
23  
24  
25  
26  
27  
28  
29  
30  
31  
32  
33  
34  
35  
36  
37  
38  
39  
40  
41  
42  
43  
44  
45  
46  
47  
48  
49  
50  
51  
52  
53  
54  
55  
56  
57  
58  
59  
60  
61  
62  
63  
64  
65

225 contents in light Rare Earth Element (LREE) and low heavy Rare Earth Element contents (HREE),  
226 resulting in steep REE patterns (La/Yb up to 70) while high-K rocks exhibit less fractionated REE  
227 patterns with HREE contents that are significantly higher than those of medium-K rocks (Fig. 7).  
228 The two rock types display different Eu anomalies with no Eu anomaly or slightly negative in  
229 the medium-K rocks and a well pronounced Eu anomaly for high-K granitoids and gneisses.  
230 Overall, medium-K<sub>2</sub>O rocks share similar chemical features with rocks of the Archean tonalite-  
231 trondhjemite-granodiorite (TTG) series, whilst high-K granitoids are similar to high-silica I-type  
232 granites. The latter plotting consistently in the field of biotite- and two-mica granites recently  
233 defined by Laurent et al. (2014) for late-Archean granites (Farina et al., 2015).  
234 Finally, leucogranitic sheets and dikes, representing ca. 10% of the bulk crystalline basement  
235 exposed in the Quadrilátero Ferrífero, display characteristic low to very low MgO + Fe<sub>2</sub>O<sub>3tot</sub>  
236 contents (0.2-1.1 wt.%) and scattered major element composition with K<sub>2</sub>O ranging from 3.8 to  
237 8.9 wt.% and silica between 71 and 76 wt.% (Fig. 6). In the SiO<sub>2</sub> vs. Al<sub>2</sub>O<sub>3</sub> diagram, they  
238 generate a quasi-linear negative trend and for equivalent silica contents they are slightly  
239 enriched in Al<sub>2</sub>O<sub>3</sub> and depleted in MgO and Fe<sub>2</sub>O<sub>3tot</sub> than both granites and gneisses (Fig. 6).  
240 The leucogranitic rocks exhibit Eu anomalies varying from slightly negative to strongly positive  
241 (Eu/Eu\* = 0.9-2.8), low REE contents and flat REE patterns resulting in low La/Yb ratios (Fig 7).

242

#### 243 4.3. Geochronology

244 A review of published U–Pb ages from the basement of the Quadrilátero Ferrífero (Table B in  
245 the Data Repository) allowed the identification of four main magmatic events (Farina et al.,  
246 2015; Lana et al., 2013; Romano et al., 2013). These periods of magmatic activity, described as  
247 the Santa Bárbara (SB), Rio das Velhas I (RVI), Rio das Velhas II (RVII) and Mamona, embody a  
248 significant part of the protracted tectonomagmatic Archean history of the Quadrilátero  
249 Ferrífero, spanning from 3220 to 2680 Ma. The first magmatic pulse, poorly preserved in the  
250 north-south elongated Santa Bárbara complex (Fig. 1), ranges from 3220 to 3200 Ma, with

1  
2  
3  
4  
5  
6  
7  
8  
9  
10  
11  
12  
13  
14  
15  
16  
17  
18  
19  
20  
21  
22  
23  
24  
25  
26  
27  
28  
29  
30  
31  
32  
33  
34  
35  
36  
37  
38  
39  
40  
41  
42  
43  
44  
45  
46  
47  
48  
49  
50  
51  
52  
53  
54  
55  
56  
57  
58  
59  
60  
61  
62  
63  
64  
65

251 these rocks representing the only Paleoproterozoic crust identified in the Quadrilátero Ferrífero so  
252 far. Most of the gneisses in the Quadrilátero Ferrífero formed during the following periods of  
253 magma production, the Rio das Velhas I and II events (Lana et al. 2013). The Rio das Velhas I  
254 period, which originally had an interval of between 2930 and 2900 Ma, has been recently  
255 expanded down to 2850 Ma by Farina et al. (2015). Similarly, new geochronological data, of  
256 Farina et al. (2015) redefine the time of the Rio das Velhas II period to between 2800 and 2760  
257 Ma. It is worth noting that, two weakly deformed plutons intruded the orthogneisses during  
258 the Rio das Velhas II event at about 2770 Ma (i.e. the Caeté and Samambaia plutons, Machado  
259 et al., 1992). The age of these granites suggest that the youngest Archean regional  
260 metamorphic event in the Quadrilátero Ferrífero occurred in the early Neoproterozoic, during the  
261 Rio das Velhas II event. The occurrence of this metamorphic event is supported by the  
262 observation that many magmatic zircon grains from the banded gneisses of the Rio das Velhas  
263 I period are overgrown by metamorphic rims yielding Rio das Velhas II ages (Lana et al., 2013).  
264 Just after the regional metamorphic event, the basement complexes underwent a new period  
265 of widespread magmatism between 2750 and 2680 Ma (Romano et al., 2013) referred to as  
266 the Mamona event by Farina et al. (2015). During this event, granites were emplaced as large  
267 batholiths and small leucogranitic veins and dikes into the pre-existing deformed crust. Finally,  
268 a volumetrically minor event of granite production accounting for less than 1% of the  
269 continental crust in the Quadrilátero occurred at ca. 2612 Ma (Romano et al., 2013).  
270 Two leucogranitic-pegmatitic dikes analysed by Machado et al. (1992) in the southern part of  
271 the Bação complex have yielded Paleoproterozoic U-Pb monazite ages (i.e. 2130 and 2122 Ma,  
272 **Table E Data Repository**). One of the dike is intrusive into the banded gneisses while the other  
273 intruded along the schistosity of the greenstone belt, a few meters away from the shear zone  
274 marking the contact between the supracrustal rocks and the basement. These ages match with  
275 the crystallization age of the Alto Maranhão suite (Noce et al., 1998; Seixas et al., 2013); a  
276 tonalitic-dioritic batholith, located on the southern edge of the Quadrilátero Ferrífero, formed

1  
2  
3  
4  
5  
6  
7  
8  
9  
10  
11  
12  
13  
14  
15  
16  
17  
18  
19  
20  
21  
22  
23  
24  
25  
26  
27  
28  
29  
30  
31  
32  
33  
34  
35  
36  
37  
38  
39  
40  
41  
42  
43  
44  
45  
46  
47  
48  
49  
50  
51  
52  
53  
54  
55  
56  
57  
58  
59  
60  
61  
62  
63  
64  
65

277 during the Rhyacian orogenesis of the South American platform (Seixas et al., 2013).  
278 Paleoproterozoic U-Pb ages were also obtained from metamorphic titanites and monazites  
279 from amphibolitic dikes (ca. 2050 Ma) and gneisses (2080-1950 Ma) in the **Bação, Bonfim and**  
280 **Belo Horizonte complexes** (Machado et al., 1992; Noce et al., 1998; Aguilar Gil et al., 2015).

## 283 **5. The Rio das Velhas Supergroup**

### 284 *5.1. Stratigraphy*

285 The metavolcanic and metasedimentary rocks of the Rio das Velhas Supergroup ( Dorr, 1969)  
286 form a typical Archean greenstone belt sequence characterized by the association between  
287 mafic and ultramafic rocks (komatiite–basalt), evolved volcanic (dacites) and volcanoclastic  
288 rocks and immature clastic sediments (Zucchetti et al., 2000; Noce et al., 2005). These rocks  
289 are metamorphosed at greenschist to lower amphibolite-facies conditions and are commonly  
290 affected by hydrothermal alteration (Ladeira et al. 1983; Zucchetti et al., 2000). Many different  
291 stratigraphic subdivision were proposed for the Rio das Velhas Supergroup (Baltazar and  
292 Zucchetti, 2007 and references therein). A first level of classification was introduced by Dorr  
293 (1969), which subdivided the greenstone belt into the Nova Lima and Maquiné groups, the  
294 former occurring at the base of the sequence and hosting the major gold deposits of the  
295 Quadrilátero Ferrífero (Fig. 3). Recently, Baltazar and Zucchetti (2007), following the approach  
296 of Eriksson et al. (1994) subdivided the Nova Lima Group into six sedimentary lithofacies  
297 associations forming four sedimentary cycles. From bottom to top these are: (i) mafic-  
298 ultramafic volcanic; (ii) volcano-chemical-sedimentary; (iii) clastic-chemical-sedimentary, (iv)  
299 volcanoclastic; (v) re-sedimented and (vi) coastal. The basal lithofacies of the Nova Lima Group  
300 is made of mafic and ultramafic lavas (Fig. 9) intercalated with minor intrusions of gabbro,  
301 anorthosite and peridotite as well as with banded iron formation, ferruginous cherts, chemical

1  
2  
3  
4  
5  
6  
7  
8  
9  
10  
11  
12  
13  
14  
15  
16  
17  
18  
19  
20  
21  
22  
23  
24  
25  
26  
27  
28  
29  
30  
31  
32  
33  
34  
35  
36  
37  
38  
39  
40  
41  
42  
43  
44  
45  
46  
47  
48  
49  
50  
51  
52  
53  
54  
55  
56  
57  
58  
59  
60  
61  
62  
63  
64  
65

302 carbonaceous sediments and rare felsic volcanoclastic rocks. The ultramafic lavas are massive  
303 and pillowed komatiites characterized by spinifex textures (Schorscher, 1978; Sichel, 1983),  
304 with layers of cumulus olivine/intercumulus orthopyroxene and a level of lahar-type breccia  
305 (Baltazar and Zucchetti, 2007). This event of mafic volcanism was followed by submarine  
306 deposition of pelites, graywackes and quartzites with intercalation of banded iron formation,  
307 dolomites, marls, carbonate-rich pelites (hosting the world-class Morro Velho gold deposit;  
308 Lobato et al., 2001) and conglomerates (i.e. lithofacies ii and iii). Volcanoclastic and  
309 resedimented volcanoclastic rocks as well as minor lava flows of dacitic composition and  
310 turbiditic graywakes form the overlying lithofacies (iv and v). It is worth noting that the minor  
311 dacitic lava flows have a TTG signature, exhibiting high Na<sub>2</sub>O and Al<sub>2</sub>O<sub>3</sub> contents (Fig. 6) and  
312 strongly fractionated Rare Earth Element patterns that are consistent with partial melting of  
313 basaltic rocks at depths where garnet is stable as a residual phase (Da Silva et al., 2000).  
314 Finally, the lithofacies at the top of the sequence (i.e. vi) is formed by sandstones with  
315 herringbone cross-bedding, ripple marks and large-scale cross-bedding. This lithofacies is  
316 restricted to a small area northwest of the Bação Complex and was probably deposited in  
317 shallow marine environment.

318 Overlying the Nova Lima Group, the Maquiné Group represents a 2000 m thick clastic  
319 association comprising conglomerates (Fig. 9) and sandstones that was described by Dorr  
320 (1969) as a flysch to molasse-type sequence, consisting of a coarsening upward succession of  
321 sandstones getting more quartz rich and conglomeratic toward the top. The Maquiné Group  
322 was divided into two formations: the basal Palmital (O'Rourke, 1957) and the upper Casa Forte  
323 (Gair, 1962). The Palmital Formation was deposited in a marine environment as proximal  
324 turbidites while the Casa Forte Formation is interpreted as a non-marine alluvial fan – braided  
325 river deposit. The contact between the Nova Lima Group and the overlying sandstones and  
326 conglomerates of the Maquiné Group is either gradational or locally unconformable and  
327 marked by fault zones (Dorr, 1969). The lack of a clear discordance between the Palmital

1  
2  
3  
4  
5  
6  
7  
8  
9  
10  
11  
12  
13  
14  
15  
16  
17  
18  
19  
20  
21  
22  
23  
24  
25  
26  
27  
28  
29  
30  
31  
32  
33  
34  
35  
36  
37  
38  
39  
40  
41  
42  
43  
44  
45  
46  
47  
48  
49  
50  
51  
52  
53  
54  
55  
56  
57  
58  
59  
60  
61  
62  
63  
64  
65

328 Formation and the top of the Nova Lima Group as well as the marine environment of  
329 deposition for the Palmital Formation led Baltazar and Zucchetti (2007) to associate this  
330 formation to the coastal association defined in the Nova Lima Group.

331

## 332 *5.2. Geochronology*

333 U-Pb ages of detrital zircon grains from the Rio das Velhas greenstone belt were determined  
334 by Machado et al. (1992, 1996), Noce et al. (2005) and Hartmann et al. (2006) using different  
335 analytical techniques such as SHRIMP, LA-ICP-MS and ID-TIMS (Table C in the Data Repository).  
336 Eight of the nine samples analysed are greywackes from the Nova Lima group while only five  
337 zircon grains were analysed for one sample collected by Machado et al. (1996) from the  
338 Maquiné Group. Three volcanoclastic graywackes from the Nova Lima Group yielded maximum  
339 deposition ages of 2792±11, 2773±7 and 2751±9 Ma, indicating ca. 40 Ma of felsic volcanism in  
340 the Quadrilátero Ferrífero (Machado et al., 1992, 1996; Noce et al., 2005). The occurrence of a  
341 Neoproterozoic felsic volcanic event is supported by a zircon <sup>207</sup>Pb/<sup>206</sup>Pb crystallization age of  
342 2772±6 Ma determined by Machado et al. (1992) for a dacitic flow intercalated within the  
343 sequence of mafic- to ultramafic volcanic rocks in the greenstone belt. Detrital zircons from  
344 two sandstones from the top of the Nova Lima Group dated by SHRIMP by Hartmann et al.  
345 (2006) gave a maximum depositional age of 2749±7 Ma.

346 U-Pb age data from detrital zircon grains in the Nova Lima Group are plotted in the frequency  
347 diagram of figure 10. In this diagram, ages that are more than 10% discordant were excluded  
348 together with spot analyses with Th/U < 0.1 as such low ratios are typical of high-grade  
349 metamorphic zircon (e.g. Rubatto et al., 2001). Detrital zircon grains from the volcanoclastic  
350 graywackes of the Nova Lima Group define a polymodal age spectrum with ages ranging from  
351 2700 to 3450 Ma. The occurrence of a large number of detrital zircon grains suggests that  
352 these rocks were not formed in an intra-oceanic arc environment, but more likely in an intra-

1  
2  
3  
4  
5  
6  
7  
8  
9  
10  
11  
12  
13  
14  
15  
16  
17  
18  
19  
20  
21  
22  
23  
24  
25  
26  
27  
28  
29  
30  
31  
32  
33  
34  
35  
36  
37  
38  
39  
40  
41  
42  
43  
44  
45  
46  
47  
48  
49  
50  
51  
52  
53  
54  
55  
56  
57  
58  
59  
60  
61  
62  
63  
64  
65

353 continental or continental-margin tectonic setting (Noce et al., 2005). A comparison of the  
354 detrital zircons age spectra of the Nova Lima Group with the ages of the main magmatic events  
355 defined by Lana et al. (2013), Romano et al., (2013) and Farina et al. (2015), leads to the  
356 following conclusions:

- 357 • The main magmatic event preserved in the metasedimentary rock record is the 2800-  
358 2760 Ma Rio Das Velhas II event,
- 359 • The second highest frequency peak is at ca. 2860 Ma matching the youngest limit of  
360 the Rio Das Velhas I event (2920-2860 Ma).
- 361 • There is a peak at ca. 3200 Ma matching the age of the Santa Bárbara event.
- 362 • The ca. 3000 Ma peak suggest an event of continental crust production that took place  
363 between the Rio Das Velhas I and Santa Bárbara magmatic events.
- 364 • Small peaks at ca. 3450 and 3550 Ma were found by Noce et al (2005) and Machado et  
365 al. (1996), respectively. The age of these peaks do not match with any of the magmatic  
366 event preserved in the basement, suggesting the existence of a pre-3200 Ma (older  
367 than the Santa Bárbara event) continental crust.

368 The limited available U–Pb age data for the Maquiné Group suggest that a continental block  
369 ranging in age from 3260 to 2877 Ma was the main source for the sandstones and  
370 conglomerates of this group (e.g., Machado et al., 1996). A recent study has associated this  
371 sedimentary sequence with the genesis of an inferred arc formed during the Rio das Velhas II  
372 event (Lana et al., 2013). **Moreira et al. (subm.)** produced geochronological U-Pb data of ca.  
373 1500 zircon grains from different units of the Maquiné Group. The new data indicate that the  
374 main source of the basin are rocks formed between 2760 and 2800 Ma (i.e. Rio das Velhas II  
375 event) and that the maximum depositional age for the Casa Forte Formation is 2730 Ma. Thus,  
376 suggesting that the basin closed after the Mamona magmatic event.



1  
2  
3  
4  
5  
6  
7  
8  
9  
10  
11  
12  
13  
14  
15  
16  
17  
18  
19  
20  
21  
22  
23  
24  
25  
26  
27  
28  
29  
30  
31  
32  
33  
34  
35  
36  
37  
38  
39  
40  
41  
42  
43  
44  
45  
46  
47  
48  
49  
50  
51  
52  
53  
54  
55  
56  
57  
58  
59  
60  
61  
62  
63  
64  
65

377 Finally, Schrank and Machado (1996a and b) dated monazite grains from the Nova Lima and  
378 upper Maquiné Groups obtaining Paleoproterozoic metamorphic ages spanning between 2080  
379 Ma to 1989 Ma (Table E, Data Repository). These data are consistent with the ages obtained  
380 for metamorphic monazite and titanite grains from the basement (Noce et al., 1998; Aguilar et  
381 al., 2015) as well as with U-Pb zircon magmatic ages from two leucocratic dikes analysed by  
382 Machado et al. (1992) in the southern part of the Bação complex.

383

## 384 **6. The Minas Supergroup**

### 385 *6.1. Main stratigraphic features*

386 The Paleoproterozoic Minas Supergroup (Dorr, 1969; Renger et al., 1995) is a ca. 6000 m-thick  
387 package of clastic and chemical rocks lying unconformably on the Archean greenstone belt  
388 (Fig. 3). According to Alkmim and Martins-Neto (2012), the Minas Supergroup can be  
389 subdivided in two sequences separated by a regional unconformity. The basal sequence,  
390 involving continental to marine sediments (Dorr, 1969; Renger et al., 1995) represents the  
391 development stage of a passive margin basin. The overlying sequence, consisting of the  
392 turbidites of the Sabará Group was interpreted as a submarine fan deposit marking the  
393 inversion of the passive margin (Machado et al., 1996; Alkmim and Marshak, 1998; Reis et al.,  
394 2002).

395 The basal continental to marine sedimentary sequence has been further subdivided into:

- 396 • A ca. 600 m-thick package of gold-uranium-bearing alluvial to marine sandstones,  
397 conglomerates and subordinate offshore pelites comprising the Tamanduá and Caraça  
398 groups (Simmons and Maxwell, 1961, Dorr, 1969). These rocks represent the rift and  
399 transitional phases of the passive margin development (Renger et al., 1995; Alkmim and  
400 Marshak, 1998);

- 1  
2  
3  
4  
5  
6  
7  
8  
9  
10  
11  
12  
13  
14  
15  
16  
17  
18  
19  
20  
21  
22  
23  
24  
25  
26  
27  
28  
29  
30  
31  
32  
33  
34  
35  
36  
37  
38  
39  
40  
41  
42  
43  
44  
45  
46  
47  
48  
49  
50  
51  
52  
53  
54  
55  
56  
57  
58  
59  
60  
61  
62  
63  
64  
65
- 401 • A 400 m-thick package of marine sediments that includes banded iron formations and  
402 carbonates of the Itabira Group (Dorr, 1969), recording the thermal subsidence stage of  
403 the continental passive margin (Alkmim and Marshak, 1998);
  - 404 • A ca. 450 m-thick pile of deltaic to shallow marine to deep water sediments (Piracicaba  
405 Group, Renger et al., 1995), consisting mainly of siliciclastic rocks with minor  
406 carbonates.

407

408 In the next sections, we discuss the main stratigraphic and geochronological features of each  
409 group. A summary of ages for the Minas Supergroup is presented **as Supplementary material**  
410 **(Table D).**

411

## 412 *6.2. Tamanduá and Caraça Groups*

413 The beginning of the rifting stage is recorded by the deposition of the Tamanduá Group and by  
414 the overlying basal unit of the Caraça Group: the Moeda Formation (Dorr, 1969). The  
415 Tamanduá Group (Simmons and Maxwell, 1961; Dorr, 1969) comprises mostly quartzites and  
416 quartz-phyllites -also referred as Cambotas Quartzite- and minor phyllitic and dolomitic  
417 itabirites at the top. The unit crops out in small and discontinuous areas, lying in contact with  
418 the Maquiné Group through an erosional unconformity (Dorr, 1969). The Caraça Group (Dorr,  
419 1959) showing great lateral extension in relation to its average thickness, encompasses  
420 quartzites, metaconglomerates (Moeda Formation) and phyllites (Batatal Formation) that  
421 overlie with angular and erosional discordance the Archean greenstone belt and conformably  
422 underlie the chemical sediments of the Itabira Group. The Moeda Formation comprises mostly  
423 quartzites. Subordinate pyritiferous and locally auriferous metaconglomerates, crop out  
424 predominantly in the northern half of the Quadrilátero Ferrífero (Dorr, 1969; Vilaça, 1981;  
425 Renger et al., 1988; Koglin et al. 2012). The average thickness of the formation is ca. 300 m,  
426 locally reaching up to 1000 m. This sequence represents a braided river system locally

1  
2  
3  
4  
5  
6  
7  
8  
9  
10  
11  
12  
13  
14  
15  
16  
17  
18  
19  
20  
21  
22  
23  
24  
25  
26  
27  
28  
29  
30  
31  
32  
33  
34  
35  
36  
37  
38  
39  
40  
41  
42  
43  
44  
45  
46  
47  
48  
49  
50  
51  
52  
53  
54  
55  
56  
57  
58  
59  
60  
61  
62  
63  
64  
65

427 alternated with deltaic to beach deposits as well as with thin deposits formed during marine  
428 transgression events (Vilaça, 1981; Canuto, 2010). The Moeda Formation exhibits significant  
429 mineralogical and grain size lateral variation. In several localities, the basal conglomerates  
430 exhibit lenticular shaped pebbles and cobbles of phyllites probably from the Nova Lima Group  
431 as well as rounded quartz and quartzite cobbles (Dorr, 1969; Koglin et al., 2012). Some of the  
432 basal fluvial metaconglomerates exhibit heavy mineral layers of detrital pyrite with economic  
433 gold concentrations (Renger et al., 1988). The Caraça cycle ends with the deposition of the  
434 Batatal Formation (Maxwell, 1968, Dorr, 1969) that conformably overlies the Moeda  
435 Formation. The contact between the two formations is commonly sharp, but locally the units  
436 can also be intergradational (Wallace, 1965). The Batatal formation consists of bluish-grey  
437 phyllites with minor metacherts, iron-formation and graphitic phyllites (Simmons, 1968)  
438 cropping out in the western and central areas of the Serra do Curral where it shows a thickness  
439 ranging from 30 to 200 meters (Dorr, 1969). The sedimentation of the Batatal Formation  
440 reflects the gradation from a marine to a coastal marine environment (Moraes, 1985),  
441 recording the transition from the rift-opening to the passive margin stage (Alkmim and  
442 Marshak, 1998).  
443 Zircon U–Pb detrital age data for the quartzites of the Caraça and Tamanduá sediments show  
444 two main age populations: 2.85-2.90 and 2.68-2.75 Ga (Machado et al., 1996; Hartmann et al.,  
445 2006; Koglin et al., 2014; Fig. 11). The age of these population peaks matches with the Rio das  
446 Velhas I and Mamona events for the genesis of the gneisses and granites of the basement. The  
447 youngest concordant zircon detrital age for a quartzite sample of the Tamanduá Group  
448 indicates a maximum age of sedimentation of  $2676 \pm 23$  Ma (Koglin et al., 2014). The  
449 deposition age for the Moeda Formation is a matter of debate. A maximum depositional age as  
450 young as  $2580 \pm 7$  Ma was proposed by Hartmann et al. (2006) based on U-Pb SHRIMP data  
451 from a zircon grain derived from a quartzite at the top of the Serra de Moeda. This  
452 depositional age is slightly younger than the deposition ages determined by Machado et al.

1  
2  
3  
4  
5  
6  
7  
8  
9  
10  
11  
12  
13  
14  
15  
16  
17  
18  
19  
20  
21  
22  
23  
24  
25  
26  
27  
28  
29  
30  
31  
32  
33  
34  
35  
36  
37  
38  
39  
40  
41  
42  
43  
44  
45  
46  
47  
48  
49  
50  
51  
52  
53  
54  
55  
56  
57  
58  
59  
60  
61  
62  
63  
64  
65

(1996) for three quartzites collected near the city of Ouro Preto, south of the Serra do Gandarela and in western flank of the Serra de Moeda ( $2606 \pm 47$  Ma,  $2649 \pm 16$  Ma and  $2651 \pm 33$  Ma, respectively). Recently, U-Pb analyses carried out on zircons grains from the southernmost tip of the Serra de Gandarela led Koglin et al. (2014) to suggest a maximum depositional age for the upper part of the Moeda Formation of  $2623 \pm 14$  Ma. In addition, Koglin et al. (2014) determined the Lu–Hf isotope composition of detrital zircon grains from metaconglomerates of the Moeda Formation (Fig.12). The zircon grains show mainly subchondritic initial  $\epsilon_{\text{Hf}}$  and large  $\epsilon_{\text{Hf}}$  variations for all the population peaks.

461

### 462 *6.3. Itabira Group*

463 The sedimentation of the Caraça shallow-water pelites (Batatal Formation) is interdigitated  
464 with rocks formed during a major marine transgression recording a period of iron-rich  
465 chemical sedimentation known as the Itabira Group (Dorr, 1969). This event led to the  
466 accumulation of more than 350 m-thick Lake Superior-type banded-iron deposit –the Cauê  
467 Formation-, and to the subsequent deposition of ca. 600 m of the stromatolite-rich carbonates  
468 of the Gandarela Formation (Fig. 3; Dorr, 1969; Babinski et al., 1995; Machado et al., 1996).  
469 The Cauê Formation (Dorr, 1969; Klein and Ladeira, 2000) or Cauê *Itabirite* –as  
470 metamorphosed rocks of the banded iron-formations are known in Brazil (the term itabirite  
471 was introduced by Eschwege in 1822) - is nowadays the economically most important unit of  
472 the Quadrilátero Ferrífero, hosting world-class hematite-rich iron ore deposits producing more  
473 than 180 Mt per year (Rosière et al., 2008). Four compositionally different lithofacies of the  
474 metamorphosed iron formations occur: siliceous, dolomitic, amphibolitic and magnetitic  
475 itabirites (Fig. 9). Rosière et al. (2008) reviewed the main features of the iron ores in the  
476 Quadrilátero Ferrífero, presenting the petrogenetic and metallogenic models proposed for the  
477 origin of these rocks. The youngest unit of the Itabira Group is the Gandarela Formation (Dorr,  
478 1969; Babinski et al. 1993). This formation is predominantly composed of dolomites,

1  
2  
3  
4  
5  
6  
7  
8  
9  
10  
11  
12  
13  
14  
15  
16  
17  
18  
19  
20  
21  
22  
23  
24  
25  
26  
27  
28  
29  
30  
31  
32  
33  
34  
35  
36  
37  
38  
39  
40  
41  
42  
43  
44  
45  
46  
47  
48  
49  
50  
51  
52  
53  
54  
55  
56  
57  
58  
59  
60  
61  
62  
63  
64  
65

479 limestones, carbonaceous phyllites and dolomitic iron-rich formation in which stromatolitic  
480 structures are preserved (Souza and Müller, 1984). This formation crops out in the Serra de  
481 Moeda, in the central part of the Serra do Curral and in the Gandarela syncline where it  
482 reaches its maximum thickness (750 meters, Dorr 1969). Its basal contact with the Cauê  
483 Formation consists of a transitional zone (up to ten meters thick) in which the dolostone is  
484 associated with the dolomitic itabirite. Babinski et al. (1995) provided an isochron Pb-Pb age of  
485  $2419 \pm 19$  Ma for a stromatolitic limestone from an intermediate member of the formation  
486 sampled from the Gandarela syncline. This age, due to the preservation of organic structures  
487 and the absence of deformation in the rocks of the Ganderela Formation, is considered to  
488 represent the sedimentation age of the carbonates.

489 The depositional age of the Cauê Formation can be bracketed between 2580 and 2420 Ma; i.e.  
490 between the maximum deposition age of the underlying Moeda Formation (Machado et al.,  
491 1996; Hartmann et al., 1996) and the age of the overlying Gandarela Formation (Babinski et al.,  
492 1995). Recently U–Pb dating of zircon grains from a metavolcanic layer sampled within the  
493 Itabira iron formation led Cabral et al. (2012) to propose a considerably earlier (2650 Ma)  
494 deposition age for this unit (Fig. 11). The interpretation of this age is controversial, since it  
495 contradicts most of the data produced so far for the underlying Caraça Group. Recently, LA-  
496 ICP-MS U-Pb dating of detrital zircon grains from a quartzite lens hosted within the Cauê  
497 Formation showed a quasi-unimodal distribution with a peak at 2795 Ma (Cassino et al., 2014).  
498 The youngest concordant zircon grain in this lens yielded an age of  $2453 \pm 18$  Ma.

#### 500 *6.4. Piracicaba Group*

501 The carbonates of the Gandarela Formation are in contact with deep-seated marine  
502 sandstones and pelites of the Piracicaba Group (Dorr et al., 1957; Dorr, 1969). This group is  
503 composed of ca. 1300 m-thick metasediments consisting of quartz-rich sandstones that

1  
2  
3  
4  
5  
6  
7  
8  
9  
10  
11  
12  
13  
14  
15  
16  
17  
18  
19  
20  
21  
22  
23  
24  
25  
26  
27  
28  
29  
30  
31  
32  
33  
34  
35  
36  
37  
38  
39  
40  
41  
42  
43  
44  
45  
46  
47  
48  
49  
50  
51  
52  
53  
54  
55  
56  
57  
58  
59  
60  
61  
62  
63  
64  
65

504 gradually fines and thins upward to mudstone and graphitic mudstone. The Piracicaba Group is  
505 subdivided into four formations that are known as the Cercadinho, Fêcho do Funil, Taboões  
506 and Barreiro formations (Fig. 3). The lowest sequence (i.e. Cercadinho Formation) comprises  
507 coarse to fine grained hematite-rich quartzites, quartzites, silvery sheen phyllites, Fe-rich  
508 phyllites as well as dolomites (Simmons, 1968; Dorr, 1969). A conglomerate containing pebbles  
509 derived from the underlying Cauê and Gandarela Formations, from which the Cercadinho  
510 Formation is separated by an erosional unconformity, marks the base of the Piracicaba Group.  
511 Detrital zircon grains from quartzites and poorly sorted conglomeratic quartzites at the base of  
512 the Cercadinho Formation, in the western part of Serra do Curral, show an Archean  
513 contribution during the initial stages of deposition of the Piracicaba Group (Mendes et al.,  
514 2014). The detrital zircon ages from these samples range between 2750 and 2900 Ma with two  
515 distinguishable peaks at 2793 Ma and 2859 Ma (Fig. 11), which correspond to the Rio das  
516 Velhas II and Rio das Velhas I events. The deposition age for the Piracicaba Group is still poorly  
517 constrained between 2420 Ma (i.e. the age of the Gandarela Formation; Babinski et al., 1995)  
518 and ca. 2100 Ma (Babinski et al., 1993). The minimum age for the Piracicaba Group (2100 Ma)  
519 was obtained by Babinski et al. (1993), by dating deformed dolomitic carbonates from the  
520 Fecho do Funil Formation. This Pb/Pb isochron age is interpreted as the metamorphic age of  
521 the rock, thus defining the minimum age of deposition for the carbonates.

522

### 523 *6.5. Sabará Group*

524 The Sabará Group is the youngest and thickest unit of the Minas Supergroup (Fig. 3),  
525 comprising up to 3.5 km-thick pile of coarsening upwards sequences of metapelites,  
526 greywackes, lithic conglomerates, and diamictites (Fig. 9; Dorr 1969; Barbosa 1979; Renger et  
527 al. 1994; Reis et al., 2002). This formation is interpreted as representing a turbiditic, submarine  
528 fan deposit formed during the inversion of the Minas Supergroup passive margin (Alkmim and

1  
2  
3  
4  
5  
6  
7  
8  
9  
10  
11  
12  
13  
14  
15  
16  
17  
18  
19  
20  
21  
22  
23  
24  
25  
26  
27  
28  
29  
30  
31  
32  
33  
34  
35  
36  
37  
38  
39  
40  
41  
42  
43  
44  
45  
46  
47  
48  
49  
50  
51  
52  
53  
54  
55  
56  
57  
58  
59  
60  
61  
62  
63  
64  
65

529 Martins-Neto, 2012). The unit is well exposed and can be mapped continuously for more than  
530 60 km along the Serra do Curral (Fig. 1).  
531 Detrital zircon ages obtained by Machado et al. (1996) for a greywacke from the Serra do  
532 Curral suggest a distinctive age distribution pattern showing a few Proterozoic ages spreading  
533 between 2100 and 2500 Ma and a well-defined peak at 2850-2900 Ma (Fig. 11). The U-Pb age  
534 distribution of detrital zircon grains in this sample is remarkably different from the age  
535 distribution of zircon grains from a felsic schist belonging to the Sabará Group, collected close  
536 to Ouro Preto. The schist, analysed by Hartmann et al. (2006) by SHRIMP, shows no  
537 Proterozoic ages and two Archean peaks at 2720 and 2900 Ma (Fig. 11). Although, Hartmann  
538 et al., (2006), reported no Proterozoic ages, a Rhyacian maximum age of deposition for the  
539 Sabará Group is confirmed by two zircon ID-TIMS U-Pb ages yielding  $2125\pm 4$  Ma (Machado et  
540 al. 1992) and  $2131\pm 5$  Ma (Machado et al., 1996). These Rhyacian ages match well with the  
541 ages obtained by Noce et al. (1998) and Seixas et al. (2013) from the Alto Maranhão suite (*ca.*  
542 2130 Ma) and associated granitoids of the Mineiro Belt (2100-2200 Ma) that bounds the  
543 Quadrilátero Ferrífero to the south. In addition, the deposition of the Sabará turbidites marks a  
544 major change in the source of Minas sediments. Paleogeographic studies (Dorr, 1969; Renger  
545 et al., 1995; Machado et al., 1996) indicate that during the genesis of the passive margin the  
546 Archean sources were located to the north. On the other hand, a non-cratonic source, located  
547 to the south and southeast, is suggested to account for the occurrence of 2100 Ma old  
548 granitoid clasts and zircons in the conglomerates of the Sabará Group (Alkmim and Martins-  
549 Neto, 2012). The turbiditic pelites, greywackes, lithic conglomerates and diamictites of the  
550 Sabará Group were interpreted as representing syn-orogenic sediments (Dorr, 1969; Renger et  
551 al., 1995; Reis et al., 2002) shed from a colliding magmatic arc and spread over an evolving  
552 foreland basin onto the São Francisco craton margin during the Rhyacian orogeny (Alkmim and  
553 Marshak, 1998; Alkmim and Martins-Neto, 2012).

554

1  
2  
3  
4  
5  
6  
7  
8  
9  
10  
11  
12  
13  
14  
15  
16  
17  
18  
19  
20  
21  
22  
23  
24  
25  
26  
27  
28  
29  
30  
31  
32  
33  
34  
35  
36  
37  
38  
39  
40  
41  
42  
43  
44  
45  
46  
47  
48  
49  
50  
51  
52  
53  
54  
55  
56  
57  
58  
59  
60  
61  
62  
63  
64  
65

## 555 7. The Itacolomi Group

556 The Itacolomi Group (Dorr, 1969), the youngest unit in the Quadrilátero Ferrífero supracrustal  
557 sequence, comprises an up to 2 km-thick section of medium- to coarse-grained quartz  
558 metasediments (Fig. 9), metaconglomerates and minor phyllites separated from the  
559 underlying Minas Supergroup by regional unconformity (Dorr, 1969; Alkmim and Martins-  
560 Neto, 2012). The occurrence of a major erosional event at the base of the unit is manifested by  
561 the polymictic nature of the metaconglomerates, in which pebbles of quartzite, itabirite and  
562 granitic rocks were recognized (Dorr, 1969). The group has a restricted areal distribution,  
563 limited to the southernmost region of the Quadrilátero Ferrífero south of Ouro Preto (Fig. 1).  
564 These rocks preserve primary sedimentary structures such as ripple marks and cross bedding  
565 and exhibit abrupt lateral changes of sedimentary facies. These features suggest that the  
566 Itacolomi Group represents interfingering marine and continental deposits. The only studies of  
567 sedimentary provenance that used U–Pb dating of detrital zircons for the Itacolomi Group are  
568 those published by Machado et al. (1996) and more recently, Hartmann et al. (2006). A  
569 summary of zircon U-Pb ages in the Itacolomi Group is presented as **Supplementary material**  
**570 (Table D)**. The two datasets show significant differences that are difficult to reconcile, as the  
571 datasets are hardly comparable. Machado et al. (1996) determined by laser ablation the U-Pb  
572 age of many detrital grains, however the age uncertainties are variable and typically large ( $1\sigma =$   
573 15-200 Ma) and the degree of concordance is not provided, therefore casting doubt about the  
574 reliability of these ages. On the other hand, Hartmann et al. (2006) used a more accurate  
575 technique (SHRIMP) and provided information about the degree of concordancy as well as on  
576 accuracy and precision. However, the database of Hartmann et al. (2006) is very limited and  
577 likely not representative as these authors analysed only seven concordant zircons. Hartmann  
578 et al. (2006) determined a maximum depositional age of  $2143\pm 16$  Ma for the Itacolomi Group  
579 in its type locality, while Machado et al. (1996) determined depositional ages that are ca. 100  
580 Ma younger (i.e.  $2039\pm 42$  Ma and  $2059\pm 58$  Ma; Fig. 11). Another difference between the two



1  
2  
3  
4  
5  
6  
7  
8  
9  
10  
11  
12  
13  
14  
15  
16  
17  
18  
19  
20  
21  
22  
23  
24  
25  
26  
27  
28  
29  
30  
31  
32  
33  
34  
35  
36  
37  
38  
39  
40  
41  
42  
43  
44  
45  
46  
47  
48  
49  
50  
51  
52  
53  
54  
55  
56  
57  
58  
59  
60  
61  
62  
63  
64  
65

581 datasets is that Machado et al. (1996) found many grains yielding  $^{207}\text{Pb}/^{206}\text{Pb}$  ages in the range  
582 2200-2500 Ma (Fig.11) which are not found by Hartmann et al. (2006). Finally, in contrast to  
583 what is observed for the underlying Sabará Group, only a subset of zircon grains from the  
584 sandstone and conglomerates of the Itacolomi Group yielded Archean ages. The large  
585 percentage of Rhyacian detrital zircons (i.e. between 2300 and 2050 Ma) in the conglomerates  
586 of the Itacolomi basins support a non-cratonic source (Machado et al., 1996; Alkmim and  
587 Marshak, 1998) suggesting that most of the sediments were derived from terrains generated  
588 during the Rhyacian orogeny. The source was probably located to the south and southeast,  
589 with the Alto Maranhão Suite (ca. 2130 Ma, Seixas, et al., 2013), Juiz de Fora (2041±7 Ma and  
590 2137±19, Noce et al., 2007) and Mantiqueira complexes (2119 ±16 to 2084±13 Ma, Noce et al.,  
591 2007) being the most suitable candidates. The Itacolomi Group is interpreted as an  
592 intermontane molasse deposit developed along the margin of the Archean nucleus of the São  
593 Francisco craton during the collapse phase of the Rhyacian orogeny (Marshak et al., 1992;  
594 Alkmim and Marshak, 1998; Alkmim and Martins-Neto, 2012).

595

## 596 **8. Mafic and intermediate dikes**

597 Mafic and intermediate intrusives occur as meter-scale blocks, boudins and lenses hosted  
598 within the gneisses as well as dikes crosscutting granites and supracrustal rocks. Carneiro  
599 (1992) and Carneiro et al. (1998) defined four groups of mafic-intermediate amphibolites in  
600 the Bonfim complex, based on field relationships, orientation as well as on textural and  
601 compositional data. Two swarms of dikes crosscut the basement and gave Neoproterozoic Sm-Nd  
602 model ages (Carneiro et al., 1998) whereas the other two groups are younger as indicated by  
603 the fact that they crosscut Paleoproterozoic metasediments and exhibit well-preserved sub-  
604 volcanic textures. Indeed, Silva et al. (1995) dated baddeleyite crystals extracted from a gabbro  
605 crosscutting the Sabará Group in the northern part of the Quadrilátero Ferrífero obtaining a

1  
2  
3  
4  
5  
6  
7  
8  
9  
10  
11  
12  
13  
14  
15  
16  
17  
18  
19  
20  
21  
22  
23  
24  
25  
26  
27  
28  
29  
30  
31  
32  
33  
34  
35  
36  
37  
38  
39  
40  
41  
42  
43  
44  
45  
46  
47  
48  
49  
50  
51  
52  
53  
54  
55  
56  
57  
58  
59  
60  
61  
62  
63  
64  
65

606 crystallization age of 1714 Ma. In the Belo Horizonte complex, unmetamorphosed tholeiitic  
607 dikes crosscutting the basement and the Supracrustal sequences yielded K/Ar feldspar ages of  
608 ca. 1000 Ma (Chavez et al., 1997). These dikes will not be described any further as this late  
609 evolution of the Quadrilátero is beyond the scope of this review.

610 The oldest population of amphibolites in the Quadrilátero is composed of mafic and  
611 intermediate boudins intruding the felsic basement. These bodies that intruded as dikes, were  
612 later rotated into parallelism with the banding in the enclosing gneisses and disrupted during  
613 ductile deformation of the basement. These boudins or lenses (hereafter “rafts”) are fine- to  
614 medium-grained, with textures varying from nematoblastic to granoblastic and geochemical  
615 affinity of within-plate tholeiite basalts. Recently, one of these rafts from the Bação complex  
616 was dated by zircon U-Pb geochronology by Lana et al. (2013) yielding a well-defined  
617 Concordia age of  $2778 \pm 8$  Ma. Titanite U-Pb ages from the same mafic raft yield  
618 Paleoproterozoic (ca. 2.1) ages suggesting resetting of the basement in the southern  
619 Quadrilátero during the Rhyacian (Aguilar et al., 2015). Farina et al. (2015) dated a dike  
620 crosscutting the ca. 2770 Ma old Samambaia tonalite in the Bonfim dome. Zircon grains from  
621 this rock gave a weighted mean  $^{207}\text{Pb}/^{206}\text{Pb}$  age of  $2719 \pm 14$  Ma, with this age matching well  
622 with the age of mafic dikes in the Uauá block in the northern São Francisco craton (Oliveira et  
623 al., 2103). These geochronological data seem to confirm the occurrence of two Neoproterozoic  
624 systems of dikes. The first swarm that emplaced at ca. 2780 Ma was successively  
625 metamorphosed and deformed together with the hosting gneisses. The second population of  
626 dikes crosscuts granitoids formed during the 2760-2680 Ma Mamona event. These dike  
627 systems are useful relative time markers allowing bracketing of the metamorphism and  
628 deformation between 2780 Ma and 2720 Ma. The tectonic significance of these Archean dikes  
629 is currently unknown as no systematic geochemical and isotopic studies were performed in the  
630 region.

631

632 **9. Main structures and structural evolution**

633 The Quadrilátero Ferrífero experienced a polyphase tectonic history that produced complex  
634 regional patterns of rock deformation (e.g., Dorr 1969; Drake and Morgan 1980; Endo 1997;  
635 Alkmim and Marshak 1998; Chemale et al 1994; Chauvet et al. 1994). This complexity, together  
636 with the lack of absolute ages dating the tectonic structures, gave rise to different and in many  
637 cases conflicting interpretations for the deformation history of the Quadrilátero. Three main  
638 sets of structures characterise the Quadrilátero Ferrífero. From the oldest to the youngest,  
639 these are:

- 640 - Northwest-verging and north–northeast-trending regional-scale folds and thrusts  
641 generating large asymmetric folds (the Gandarela syncline, Conceição anticline, Itabira  
642 synclinorium) and the steeply dipping to overturned Serra do Curral homocline (e.g.,  
643 Pomerene, 1964; Dorr, 1969; Pires, 1979; Marshak et al., 1992; Alkmim & Marshak,  
644 1998; Fig. 1).
- 645 - Extensional structures related to the formation of a typical dome-and-keel province; in  
646 which troughs of deformed and metamorphosed Paleoproterozoic supracrustal rocks  
647 surround domes of Archean basement (e.g., Belo Horizonte, Caeté, Bação complexes;  
648 Chemale et al., 1991, 1994; Alkmim & Marshak, 1998).
- 649 - West verging thrust folds reactivating and overprinting pre-existent structures in the  
650 region east of a north-trending line that follows the west edge of the Moeda syncline  
651 (Fig.1; Chemale et al., 1994).

652 According to Alkmim and Marshak (1998), these structures correspond to three kinematic  
653 phases that affect the rocks of both the Rio das Velhas and Minas Supergroups. The maximum  
654 age of formation of the oldest structures is constrained by the deposition age of the top of the  
655 Minas Supergroup: the Sabará group. This 3.5 km-thick flysch sequence that has a maximum

1  
2  
3  
4  
5  
6  
7  
8  
9  
10  
11  
12  
13  
14  
15  
16  
17  
18  
19  
20  
21  
22  
23  
24  
25  
26  
27  
28  
29  
30  
31  
32  
33  
34  
35  
36  
37  
38  
39  
40  
41  
42  
43  
44  
45  
46  
47  
48  
49  
50  
51  
52  
53  
54  
55  
56  
57  
58  
59  
60  
61  
62  
63  
64  
65

656 deposition age of 2130 Ma (Machado et al., 1996) is involved in northwest-verging folding. This  
657 age constraint led Alkmim and Marshak (1998) to interpret the northwest-verging folds and  
658 thrusts as a fold and thrust belt formed shortly after the deposition of the Sabará Group in the  
659 foreland of a Rhyacian collisional orogeny. This event, however, did not generate a strong  
660 foliation.

661 The second structures relate to the formation of the dome-and-keel geometry of the  
662 Quadrilátero. The contacts between granitic-gneissic complexes and the Supracrustal  
663 sequences are tectonic, marked by thrusts and/or normal faults, and by ductile shear zones  
664 showing variable sense of displacement (Hippertt et al., 1992; Machado et al., 1996; Alkmim &  
665 Marshak, 1998). For instance, the enveloping shear zones of the Bonfim and Belo Horizonte  
666 domes show normal sense kinematic indicators (Hippertt et al., 1992), while the shear sense  
667 observed in the contact zone of the Bação and Caeté domes varies between reverse, reverse-  
668 oblique and strike-slip (Marshak and Alkmim, 1989; Hippertt, 1994; Endo, 1997). Kinematic  
669 indicators in supracrustal rocks clearly indicate supracrustal-side-down displacement (Marshak  
670 et al., 1997) supporting an extensional event (Hippertt et al., 1992). Metamorphic aureoles in  
671 the supracrustal rocks at the contact with the domes have different thickness (Pomerene,  
672 1964; Herz, 1978; Carneriro, 1992; Jordt-Evangelista et al., 1992; Marshak et al., 1992, 1996).  
673 The dome-border shear zones and their related metamorphic aureoles overprint the foliation  
674 of Archean gneisses as well as the early regional lower greenschist-facies metamorphism and  
675 the foliation, folds and faults in the supracrustal sequence. This evidence indicates that the  
676 doming event post-dated the northwest-verging thrust and associated syncline folds (Marshak  
677 et al., 1992; Alkmim and Marshak, 1998). Syn-shear garnets formed in a dome-border shear  
678 zone in rock of the Minas Supergroup gave a Sm–Nd age of  $2095 \pm 65$  Ma (Marshak et al.,  
679 1997). This age, that is consistent with titanite and monazite U–Pb metamorphic ages obtained  
680 in the basement (Machado et al., 1992; Schrank and Machado, 1996a, b; Aguilar et al., 2015),

1  
2 681 suggests that dome emplacement occurred during the extensional collapse of the Rhyacian  
3 682 orogen.

4  
5 683 Finally, the collisional and extensional structures described were overprinted and reactivated  
6  
7 684 by a series of west-verging thrust faults and associated structures, attributed to the  
8  
9 685 Neoproterozoic Brasiliano event (630 to 490 Ma; e.g., Endo and Fonseca, 1992; Chemale et al.,  
10  
11 686 1994; Alkmim and Marshak, 1998). West-verging structures including penetrative east-  
12  
13 687 southeast-dipping schistosity, north-trending folds and a north–south-trending crenulation  
14  
15 688 lineation are observed east of a north-trending line that follows the west edge of the Moeda  
16  
17 689 syncline and cuts northwards across the Serra do Curral (i.e. the Brasiliano front). West of this  
18  
19 690 front, the Brasiliano tectonism generates northeast-trending dextral strike-slip shear zones  
20  
21 691 (Alkmim and Marshak, 1998).

22  
23  
24  
25  
26  
27 692

## 28 29 30 693 **10- Discussion: models and open problems**

31  
32  
33 694 In this section we discuss the evolution of the Quadrilátero Ferrífero from the genesis of the  
34  
35 695 continental crust in the Paleoproterozoic to the Orosirian Period. In addition, we present a series  
36  
37 696 of unresolved questions relative to the genesis and evolution of the Quadrilátero Ferrífero.

38  
39  
40  
41 697

### 42 43 44 698 *10.1. Building up the continental crust: the Paleo- to Mesoarchean rock record*

45  
46  
47 699 The oldest preserved rocks in the Quadrilátero Ferrífero are banded gneisses from the Santa  
48  
49 700 Bárbara complex that formed at the Paleo-Mesoarchean boundary (i.e. 3200 Ma, Lana et al.,  
50  
51 701 2013). Unfortunately, very little study has been conducted on these rocks so that the Paleo-  
52  
53 702 Mesoarchean rock record of the Quadrilátero Ferrífero remains enigmatic. The occurrence of  
54  
55 703 these gneisses in the region provide various lines of evidence for the generation of a  
56  
57 704 considerable volume of continental crust during the Paleoproterozoic and Late Mesoarchean  
58  
59  
60  
61  
62  
63  
64  
65

1  
2  
3  
4  
5  
6  
7  
8  
9  
10  
11  
12  
13  
14  
15  
16  
17  
18  
19  
20  
21  
22  
23  
24  
25  
26  
27  
28  
29  
30  
31  
32  
33  
34  
35  
36  
37  
38  
39  
40  
41  
42  
43  
44  
45  
46  
47  
48  
49  
50  
51  
52  
53  
54  
55  
56  
57  
58  
59  
60  
61  
62  
63  
64  
65

705 (Lana et al., 2013). Firstly, zircon grains yielding 3000–3400 Ma ages occur as inherited  
706 components in a limited number of gneisses dated by Lana et al. (2013) and represent a  
707 significant subset in the detrital spectra of the greenstone belt succession and the Minas  
708 Supergroup (Figs. 10 and 11). In particular, minor peaks at ca. 3200 Ma occur in the Tamanduá,  
709 Caraça, Itabira and Piracicaba Groups (Fig. 11) as well as in the greenstone belt in both the  
710 Nova Lima (Fig. 10) and Maquiné groups (Moreira et al., 2015). Secondly, Sm–Nd model ages  
711 for Neoproterozoic gneisses and granites in the Bonfim complex resulted in ages of up to 3300 Ma  
712 (Teixeira et al., 1996). Finally, most of the detrital zircon grains from the Moeda Formation  
713 have subchondritic initial  $\epsilon_{\text{Hf}}$  values (Fig. 12) resulting in calculated depleted mantle model  
714 ages varying from 3200 to 3600 Ma (Koglin et al., 2014). These model ages are in good  
715 agreement with those calculated by Albert et al. (2015) for magmatic zircon crystals in gneisses  
716 and granitoids from the Bonfim complex. Taken together these geochronological and isotopic  
717 data advocate for the existence of a large segment of Paleoproterozoic continental crust in the  
718 Quadrilátero Ferrífero. This crust was probably reworked and eroded during the subsequent  
719 episodes of magmatic and tectonic activity.

720 Recently, Farina et al. (2015) compared the composition of gneisses and granitoids from the  
721 Quadrilátero Ferrífero with TTGs from other cratons and experimental melts produced by  
722 fluid-absent melting of tonalites. Medium-K rocks are significantly more silica- and  $\text{K}_2\text{O}$ -rich  
723 and less  $\text{Na}_2\text{O}$ - and  $\text{Al}_2\text{O}_3$ -rich than typical TTGs (Fig. 6) and show intermediate compositions  
724 between TTGs and experimental melt obtained through fluid-absent partial melting of TTG  
725 sources such those used as starting material by Watkins et al. (2007). Based on whole-rock  
726 chemical arguments, Farina et al. (2015) suggested that medium-K banded gneisses and  
727 granitoids formed by mixing between a TTG-like melt produced by partial melting of basaltic  
728 oceanic crust and a melt derived by reworking of the continental crust. The occurrence of a  
729 recycled crustal component in the genesis of the medium-K rocks formed during the Rio Das  
730 Velhas I and II magmatic events is supported by the negative  $\epsilon_{\text{Hf}}$  composition displayed by both

1  
2  
3  
4  
5  
6  
7  
8  
9  
10  
11  
12  
13  
14  
15  
16  
17  
18  
19  
20  
21  
22  
23  
24  
25  
26  
27  
28  
29  
30  
31  
32  
33  
34  
35  
36  
37  
38  
39  
40  
41  
42  
43  
44  
45  
46  
47  
48  
49  
50  
51  
52  
53  
54  
55  
56  
57  
58  
59  
60  
61  
62  
63  
64  
65

731 detrital zircons in the Moeda Formation (Koglin et al., 2014) and magmatic zircon crystals in  
732 gneisses and granitoids (Albert et al., 2015). A subset of detrital zircon in the Moeda Formation  
733 (< 10% of the grains) and magmatic zircon from a few gneisses sampled in the Bação complex  
734 show superchondritic Hf isotopic compositions suggesting that juvenile crust was also formed  
735 during the Meso- and Neoproterozoic Rio das Velhas I and II magmatic events (Koglin et al., 2014;  
736 Albert et al., 2015).

737

### 738 *10.2. The record of plate tectonics: the Meso-Neoproterozoic*

739 Two significant changes occurred in the Quadrilátero Ferrífero during the early Neoproterozoic,  
740 between ca. 2800 and 2700 Ma. Firstly, high-K granites similar to post-Archean high-silica I-  
741 type granites were produced, largely replacing medium-K granitoids and gneisses; the latter  
742 showing chemical affinity similar to TTGs and representing the volumetrically dominant rocks  
743 produced during the Rio das Velhas I and II events (ca. 2920-2760 Ma). Secondly, mature  
744 sedimentary sequences emerged and were deposited in the Rio das Velhas greenstone belt  
745 forming the 2000 m-thick association of conglomerates and sandstones of the Maquiné Group.  
746 We argue that a model involving subduction of oceanic crust and subsequent continental  
747 collision between two continental blocks account for these two major changes explaining  
748 coherently most of the Neoproterozoic evolution of the Quadrilátero Ferrífero. The model that is  
749 illustrated in figure 13 has been proposed to explain the late-Archean geodynamic evolution of  
750 many other terranes worldwide (e.g., Percival et al., 2006; Laurent et al., 2014).

751 In the Quadrilátero, medium-K rocks were produced during the Rio das Velhas I and II events  
752 (2920-2850 and 2800-2760 Ma). These rocks have chemical composition suggesting mixing  
753 between magmas derived by partial melting of an oceanic crust and magmas derived by crustal  
754 reworking. These compositions can be generated by significant interaction between melts  
755 derived by melting a subducting oceanic slab and an upper plate formed by a Meso-

1  
2  
3  
4  
5  
6  
7  
8  
9  
10  
11  
12  
13  
14  
15  
16  
17  
18  
19  
20  
21  
22  
23  
24  
25  
26  
27  
28  
29  
30  
31  
32  
33  
34  
35  
36  
37  
38  
39  
40  
41  
42  
43  
44  
45  
46  
47  
48  
49  
50  
51  
52  
53  
54  
55  
56  
57  
58  
59  
60  
61  
62  
63  
64  
65

756 Paleoproterozoic continental nucleus. In this scenario, clastic sediments from the upper-plate  
757 eroded and deposited in a back arc basin (i.e the Maquiné Group) and volcanic rocks with TTG-  
758 affinity erupted forming dacitic flows in the greenstone belt.

759 The granitoids formed during the Rio das Velhas II event were readily deformed and  
760 metamorphosed between 2780 and 2730 Ma as indicated by the age of the earliest granites  
761 emplaced in the Bação, Bonfim and Belo Horizonte complexes (Machado et al., 1992, Romano  
762 et al., 2013, Farina et al., 2015). During these ca. 50 Ma of metamorphism the medium-K  
763 granitoids were deformed and transformed into banded gneisses and leucogranitic sheets and  
764 mafic/intermediate dikes were emplaced and rotated into parallelism with the banding in the  
765 gneisses. The pressure and temperature conditions attained during the metamorphic event are  
766 not constrained, but the occurrence of migmatites suggest that the basement reached locally  
767 granulite-facies conditions (Alkmim and Marshak, 1998). We suggest that this high-grade  
768 metamorphic event records the collision between two continental blocks. During crustal  
769 thickening, fertile metasedimentary rocks were buried. Then, thermal relaxation and extension  
770 following lithospheric delamination triggered the upwelling of the asthenosphere heating up  
771 the continental crust and inducing partial melting. High-K granites and crosscutting mantle-  
772 derived dikes form in this syn- to late-collisional geodynamic environment. Based on whole-  
773 rock chemical arguments, Farina et al. (2015) suggested that high-K granites in the  
774 Quadrilátero were produced by low degree of melting of metasedimentary sources deposited  
775 during the Rio das Velhas II event. In this scenario, the transition between medium-K and high-  
776 K granitoids reflects a change in the sources undergoing melting.

777 It is worth noting that during the Neoproterozoic, the northern (i.e. the Belo Horizonte complex)  
778 and southern (the Bação and Bonfim complexes) portions of the Quadrilátero Ferrífero  
779 experienced different magmatic evolutions. In the southern portion, medium-K granitoids  
780 emplaced for ca. 20 Ma (2790-2770 Ma) after the metamorphic peak and were then replaced



1  
2  
3  
4  
5  
6  
7  
8  
9  
10  
11  
12  
13  
14  
15  
16  
17  
18  
19  
20  
21  
22  
23  
24  
25  
26  
27  
28  
29  
30  
31  
32  
33  
34  
35  
36  
37  
38  
39  
40  
41  
42  
43  
44  
45  
46  
47  
48  
49  
50  
51  
52  
53  
54  
55  
56  
57  
58  
59  
60  
61  
62  
63  
64  
65

781 by high-K monzogranite and syenogranite with composition of late Archean biotite and two-  
782 mica granites (Farina et al., 2015). This rather sharp compositional change was not recorded in  
783 the Belo Horizonte complex where the ca. 2750-2720 Ma massive granitic batholiths (Pequi  
784 and Florestal, Fig. 1) have TTG-affinity. In the Belo Horizonte complex, minor bodies of high-K  
785 granites (e.g. the Santa Luzia granite) were only emplaced at ca. 2700 Ma (Noce et al., 1997).

786 The emplacement of high-K granites during the Mamona magmatic event marks the  
787 stabilization of the southern São Francisco craton. This probably occurred because the  
788 emplacement of high-K magmas at shallow level in the crust concentrated heat-producing  
789 elements (e.g. K, Th, U) in the upper crust, leaving the middle crust thermally stable (e.g.,  
790 Sandiford and McLaren, 2002). In addition, partial melting of the continental crust left the  
791 lower crust dry (refractory) and therefore more resistant to future episodes of partial melting  
792 (Romano et al., 2013).

793

### 794 *10.3. Evolution of the Minas Basin*

795 The rocks of the Minas Supergroup represents a passive-margin to syn-orogenic sedimentary  
796 package tracking the operation of a Wilson cycle between ca. 2.6 and 2.0 Ga (Alkmim and  
797 Marshak, 1998). The development of the Minas passive margin took place in the time interval  
798 between approximately 2600 and 2400 Ma (i.e. between the deposition of the Moeda and  
799 Gandarela formations; Babinski et al., 1995; Koglin et al., 2014) along the borders of the São  
800 Francisco and Congo cratons. The clastic metasedimentary rocks, forming the lowest part of  
801 the Minas Supergroup (the Tamanduá and Caraça groups), were deposited during the early  
802 subsidence of the precursor passive margin basin. The intermediate Itabira Group that is  
803 composed of the Cauê Banded Iron Formation, hosting the valuable iron ore deposits of the  
804 Quadrilátero Ferrífero, and of the limestones of the Gandarela Formations, mark the thermally  
805 subsiding stage of the Minas Basin (Alkmim and Martins-Neto, 2012). Finally, clastic immature

1  
2  
3  
4  
5  
6  
7  
8  
9  
10  
11  
12  
13  
14  
15  
16  
17  
18  
19  
20  
21  
22  
23  
24  
25  
26  
27  
28  
29  
30  
31  
32  
33  
34  
35  
36  
37  
38  
39  
40  
41  
42  
43  
44  
45  
46  
47  
48  
49  
50  
51  
52  
53  
54  
55  
56  
57  
58  
59  
60  
61  
62  
63  
64  
65

806 and flysch-like metasedimentary rocks of the uppermost Sabará Group, marks the inversion of  
807 the basin representing syn-orogenic sediments shed from a colliding magmatic arc (Dorr 1969;  
808 Barbosa 1979; Renger et al. 1995). The Sabará Group contains detrital zircon grains as young as  
809  $2125 \pm 4$  Ma (Machado et al., 1992); i.e. 300 Ma younger than the age of the underlying units  
810 of the Minas Supergroup. This marks a significant change in both the depositional setting and  
811 sediment source compared to the older Minas units that mainly derived from Archean  
812 material. The Sabará turbidites are a submarine fan deposit interpreted as having formed  
813 either as a syn-orogenic deposit scraped off from an active magmatic arc (Hartmann et al.  
814 2006) or as a foreland basin (Machado et al., 1996).

815

#### 816 *10.4. The Minas accretionary orogeny*

817 The regional setting of the Quadrilátero Ferrífero is dominated by two set of structures: i)  
818 northwest-verging and north–northeast-trending regional-scale folds and thrusts with  
819 associated low- to medium-grade metamorphism affecting the supracrustal rocks and ii)  
820 gneiss-granitic domes surrounded by elongate keels of polydeformed supracrustal rocks (i.e  
821 dome-and-keel structure). These structures formed in the Paleoproterozoic as indicated by the  
822 depositional age of the Sabará Group (2125 Ma; Machado et al., 1996), which is involved in the  
823 folding and thrusting, as well as by the age of the dome-related metamorphic contact aureole  
824 (ca. 2095 Ma; Marshak et al., 1997). The fold-and thrust belt formed in the Paleoproterozoic  
825 during the collision between the nuclei of the present-day São Francisco and Congo cratons  
826 (Alkmim and Martins-Neto, 2012). In the southern portion of the São Francisco craton, the  
827 continental collision between these two plates generated the Mineiro Belt and the adjoining  
828 Mantiqueira and Juiz de Fora complexes (Teixera et al., 2015). The Mineiro Belt, bordering the  
829 Quadrilátero Ferrífero to the south, is a km-wide corridor of polydeformed Archean gneisses  
830 and greenstone belt remnants intruded by 2350–2000 Ma granitoids (Seixas et al., 2012). This

1  
2  
3  
4  
5  
6  
7  
8  
9  
10  
11  
12  
13  
14  
15  
16  
17  
18  
19  
20  
21  
22  
23  
24  
25  
26  
27  
28  
29  
30  
31  
32  
33  
34  
35  
36  
37  
38  
39  
40  
41  
42  
43  
44  
45  
46  
47  
48  
49  
50  
51  
52  
53  
54  
55  
56  
57  
58  
59  
60  
61  
62  
63  
64  
65

831 belt was generated through successive accretion of oceanic and continental arcs that were  
832 active during the Paleoproterozoic and then final collision with the São Francisco craton,  
833 representing the foreland of the belt (Teixeira et al., 1996; Alkmim and Marshak, 1998; Ávila et  
834 al., 2010). This event is recorded in the basement by monazite and titanite crystals yielding  
835 2100-1950 Ma U-Pb metamorphic ages (Machado et al., 1992; Schrank and Machado, 1996a,  
836 b; Aguilar et al., in prep). The tectonomagmatic event affecting the southern São Francisco  
837 craton, usually referred to as the Transamazonian event (e.g., Machado et al., 1996), has been  
838 named by Teixeira et al. (2015) the Minas accretionary orogeny.

839 In the Orosirian, after the formation of the fold-and thrust belt the Quadrilátero underwent  
840 orogenic collapse, resulting in the deposition of the alluvial sandstones, conglomerates and  
841 pelites of the Itacolomi Group and development of the dome-and-keel structure (Alkmim and  
842 Marshak, 1998). The large percentage of Rhyacian detrital zircons (i.e. between 2300 and 2050  
843 Ma) in the conglomerates of the Itacolomi basins support a non-cratonic source (Machado et  
844 al., 1996; Alkmim and Marshak, 1998) suggesting that most of the sediments were derived  
845 from terrains generated during the Minas accretionary orogeny.

846 At a regional scale, the Minas accretionary orogeny correlates with the tectonic-magmatic  
847 events recognized in the Eastern Bahia belt in the northern portion of the São Francisco craton  
848 (Teixeira et al., 2015). These events seem to reflect the assembly of a supercontinent during  
849 the Orosirian period, the Atlantica supercontinent (Rogers, 1996), followed by Columbia  
850 (Rogers and Santosh, 2004; Zhao et al., 2004), whose reconstructions, though not fully  
851 accomplished, have progressed significantly in the last few years.

852

### 853 *10.5. Questions for future research*

854 Recently, new geochronological data helped improve our understanding of the ca. 1.5 Ga of  
855 evolution of the Quadrilátero Ferrífero (Lana et al., 2013, Romano et al., 2013, Mendes et al.,

1  
2  
3  
4  
5  
6  
7  
8  
9  
10  
11  
12  
13  
14  
15  
16  
17  
18  
19  
20  
21  
22  
23  
24  
25  
26  
27  
28  
29  
30  
31  
32  
33  
34  
35  
36  
37  
38  
39  
40  
41  
42  
43  
44  
45  
46  
47  
48  
49  
50  
51  
52  
53  
54  
55  
56  
57  
58  
59  
60  
61  
62  
63  
64  
65

856 2014; Farina et al; 2015). However, many open questions remain to be solved. The list of  
857 queries that follows is not aimed to be exhaustive, but we hope it could serve as a guide for  
858 future studies.

859 • What are the metamorphic conditions attained by the basement during the  
860 Neoproterozoic metamorphic event? Did the basement undergo extensive partial  
861 melting between 2780 and 2730 Ma?

862 • During the Neoproterozoic Mamona event, TTG-like granitoids emplaced in the Belo  
863 Horizonte complex while high-K granites were generated in the Bação and Bonfim  
864 complexes. Why magmas with different chemical affinity formed at the same time in  
865 the northern and southern portion of the Quadrilátero Ferrífero? Moreover, what is  
866 the chemical composition of gneisses and granitoids in the Santa Bárbara and Caeté  
867 complexes?

868 • Metaluminous Mg- Fe- and K-rich monzodiorite and granodiorites forming the  
869 sanukitoid series are regarded as markers of Archean subduction (Martin et al., 2009)  
870 and typify the late Archean evolution of many cratons (e.g. Laurent et al., 2014).  
871 Magmatic rocks with sanukitoid affinity were not described in the Quadrilátero  
872 Ferrífero. How does the proposed model of Neoproterozoic subduction-collision for the  
873 Quadrilátero account for the lack of sanukitoids?

874 • What is the age and tectonic significance of the different mafic-intermediate dike  
875 swarms crosscutting the basement and the supracrustal sequences? In particular, what  
876 is the chemical composition of the two populations of Neoproterozoic dikes and what do  
877 they tell us about the geodynamic evolution of the Quadrilátero Ferrífero?

878 • What is the age and tectonic significance of the unconformity bounded Piracicaba  
879 Group, whose depositional age is still poorly constrained?

880 • Why are the U-Pb depositional age and age distribution obtained by Machado et al.  
881 (1996) and Hartmann et al., (2006) for the rocks of the Sabará Groups so different (Fig.

1  
2  
3  
4  
5  
6  
7  
8  
9  
10  
11  
12  
13  
14  
15  
16  
17  
18  
19  
20  
21  
22  
23  
24  
25  
26  
27  
28  
29  
30  
31  
32  
33  
34  
35  
36  
37  
38  
39  
40  
41  
42  
43  
44  
45  
46  
47  
48  
49  
50  
51  
52  
53  
54  
55  
56  
57  
58  
59  
60  
61  
62  
63  
64  
65

882 11)? Does this discrepancy reflect the fact that the samples were collected from  
883 different localities and/or different stratigraphic positions? Ultimately, what is the  
884 depositional age and age distribution of the turbidites of the Sabará Group?

885 • Monazite and titanites grains from the basement gave Rhyacian U-Pb ages, while no  
886 metamorphic zircon crystals/overgrowths yielded non-Archean ages. What are the  
887 metamorphic conditions attained by the basement during the Minas orogeny? What is  
888 the geographic extent of the Rhyacian metamorphic overprint? Why no magmatism  
889 was produced in the Quadrilátero Ferrífero during the continental collision between  
890 the proto São Francisco and Congo cratons?

891

892

893

894

895

896 FIGURES

897 **Figure 1.** Geological map of the Quadrilátero Ferrífero modified after Alkmim and Marshak  
898 (1998). Batholith and **pluton abbreviations**: F- Florestal, M- Mamona, P- Pequi, Sa- Samambaia;  
899 SN- Souza-Noschese. Inset: tectonic sketch of the São Francisco craton showing the location of  
900 **the bordering Brasiliano orogenic belts as well as of the Paleoproterozoic Mineiro Belt**

901 **Figure 2.** Timeline showing the main historical events and geological discoveries in Brazil from  
902 the first colonization until today.

903 **Figure 3.** Stratigraphic column of the supracrustal sequences in Quadrilátero Ferrífero.  
904 Modified after Dorr (1969) and Alkmim and Marshak (1998).

1  
2  
3  
4  
5  
6  
7  
8  
9  
10  
11  
12  
13  
14  
15  
16  
17  
18  
19  
20  
21  
22  
23  
24  
25  
26  
27  
28  
29  
30  
31  
32  
33  
34  
35  
36  
37  
38  
39  
40  
41  
42  
43  
44  
45  
46  
47  
48  
49  
50  
51  
52  
53  
54  
55  
56  
57  
58  
59  
60  
61  
62  
63  
64  
65

905 **Figure 4.** Field photographs of the basement. (a) Leucogranitic sheets and dikes hosted within  
906 a banded gneiss, Bação Complex. (b) Banded gneiss hosting cm-scale leucogranitic sheets  
907 following the gneissosity, Bação Complex. (c) Leucogranitic sheets in a gneiss crosscut by a late  
908 fine-grained leucocratic dike. (d) meter-scale xenolith of banded gneiss hosted within medium-  
909 granite granites, Bação Complex. (e) Coarse-grained granodiorite, Mamona batholith, Bonfim  
910 Complex. (f) Contact between biotite-rich and plagioclase–quartz–biotite granites crosscut by a  
911 leucogranitic dike, Belo Horizonte complex.

912 **Figure 5.** Normative An-Ab-Or triangle (O'Connor, 1965) showing the composition of gneisses,  
913 granites and leucogranites as well as the composition of Rio das Velhas dacites. The field for  
914 Archean TTGs is from Moyen and Martin, (2012). Data are from Gomes (1985), Carneiro et al.  
915 (1992), Noce et al. (1997), Da Silva et al. (2000) and Farina et al. (2015).

916 **Figure 6.** Harker diagrams for the igneous rocks of the Quadrilátero Ferrífero: (a) SiO<sub>2</sub> vs.  
917 Al<sub>2</sub>O<sub>3</sub>, (b) SiO<sub>2</sub> vs. K<sub>2</sub>O. Grey dots are TTGs from Moyen, 2011. In (c), histogram showing the  
918 frequency of K<sub>2</sub>O/Na<sub>2</sub>O values exhibited by the rocks of the Quadrilátero Ferrífero. The bin  
919 width used is 0.2. The height of the bars represents the number of samples having the  
920 corresponding K<sub>2</sub>O/Na<sub>2</sub>O value.

921 **Figure 7.** Average chondrite-normalized REE patterns for high-K granites and medium-K  
922 gneisses and granitoids. The trace element pattern for high-K granites is obtained averaging  
923 the composition of eleven samples, patterns for medium-K gneisses and granitoids are from  
924 fifteen and sixteen samples, respectively. Data are from Farina et al. (2015). The field of TTGs is  
925 drawn using the composition of high- medium- and low-pressure TTGs (Moyen, 2011).  
926 Normalization values are from McDonough and Sun (1995).

927  
928 **Figure 8.** Timeline showing <sup>207</sup>Pb/<sup>206</sup>Pb zircon ages for intrusive and volcanic rocks of the  
929 Quadrilátero Ferrífero. Circles, squares, diamonds and triangles indicate the Bação, Bonfim,

1  
2  
3  
4  
5  
6  
7  
8  
9  
10  
11  
12  
13  
14  
15  
16  
17  
18  
19  
20  
21  
22  
23  
24  
25  
26  
27  
28  
29  
30  
31  
32  
33  
34  
35  
36  
37  
38  
39  
40  
41  
42  
43  
44  
45  
46  
47  
48  
49  
50  
51  
52  
53  
54  
55  
56  
57  
58  
59  
60  
61  
62  
63  
64  
65

930 Belo Horizonte and Santa Bárbara complexes, respectively. White and dark grey symbols are  
931 for high and medium-K rocks, respectively. In black, mafic and intermediate dikes and  
932 metamorphic zircon ages. The vertical light grey fields indicate the different magmatic events:  
933 SB- Santa Barbara RdV I- Rio das Velhas I; RdV II- Rio das Velhas II; Mam- Mamona. Data are  
934 from Romano et al., 2013; Lana et al., 2013; Machado and Carneiro, 1992; Machado et al.,  
935 1992; Noce et al., 1998; Noce et al., 1997; Chemale et al., 1993; Noce et al., 2005.

936 **Figure 9.** Field photographs of the supracrustal rocks. (a) Komatiite showing spinifex structure,  
937 basal portion of the Nova Lima Group;. (b) Metabasalt with deformed pillow structure, basal  
938 portion of the Nova Lima Group; (c) Polymictic conglomerate of the Maquiné group containing  
939 stretched clasts. (d) Cauê Itabirite showing the typical intercalation of hematite and quartz-  
940 rich bands; (e) Conglomerate of the Sabará Group containing clasts of quartzite, gneisses,  
941 granites and banded iron formation embedded in a chlorite-rich matrix; (f) Quartz  
942 metasandstone of the Itacolomi Group showing crossbedding. Crossbedding sets are marked  
943 by concentration of heavy minerals, especially iron oxides. The pens in (b), (c), (d) and (e) are  
944 14 cm long.

945  
946 **Figure 10.** Frequency histogram showing the age distribution of detrital zircon grains in the  
947 rocks of the Rio das Velhas Supergroup. The probability curve is produced considering 109 U–  
948 Pb analyses from Machado et al., 1992; Machado et al., 1996; Noce et al., 2005; Hartmann et  
949 al., 2006. Maximum discordance accepted 10%. Analyses with Th/U<0.1 were excluded.  
950 Vertical bands mark the age of the main magmatic events in the basement.

951 **Figure 11.** Frequency histogram for the Minas Supergroup. Histograms and Probability Density  
952 plots for the available U-Pb zircon ages of the Minas Supergroup and Itacolomi Group. Age  
953 display software (Sircombe, 2004) was used to build the graphs and evaluate the data. All

1  
2  
3  
4  
5  
6  
7  
8  
9  
10  
11  
12  
13  
14  
15  
16  
17  
18  
19  
20  
21  
22  
23  
24  
25  
26  
27  
28  
29  
30  
31  
32  
33  
34  
35  
36  
37  
38  
39  
40  
41  
42  
43  
44  
45  
46  
47  
48  
49  
50  
51  
52  
53  
54  
55  
56  
57  
58  
59  
60  
61  
62  
63  
64  
65

954 weighted zircon data was 95% concordant (excepting data from Machado et al. 1996) and  
955 treated as sigma-1 errors.

956 **Figure 12.** Results of U–Pb and Lu–Hf spot analyses of detrital zircon from the  
957 metaconglomerates and quartzites of the Moeda Formation presented in a  $\epsilon_{\text{Hf}(t)}$  versus  
958  $^{207}\text{Pb}/^{206}\text{Pb}$  age diagram. Data are from Koglin et al. (2014). Vertical grey bars mark the main  
959 magmatic-metamorphic events in the Quadrilátero Ferrífero. Crustal evolution trends are  
960 determined using a  $^{176}\text{Lu}/^{177}\text{Hf}$  of 0.0113 for the average continental crust.

961 **Figure 13.** Sketch of the geodynamic evolution of the Quadrilátero Ferrífero during the Rio Das  
962 Velhas I, Rio Das Velhas II and Mamona periods. In the 2920-2850 Ma cartoon, we tentatively  
963 propose that the continental crust formed by multiple accretion of island-arcs. During the Rio  
964 das Velhas II period, the subduction of an oceanic crust under a continental block led to the  
965 formation of medium-K granitoids by mixing between two components: melts derived by  
966 partial melting of the mafic oceanic crust and melts derived by recycling of older continental  
967 crust. During this event, volcanic rocks erupted above the ultramafic-mafic sequence of the  
968 Nova Lima Group and mantle-derived magmas intruded the basement. Finally, during the  
969 Mamona event, two continental blocks collided. Slivers of metasediments were buried and  
970 started melting producing high-K granites and clastic sediments were deposited forming the  
971 Maquiné Group. Modified and adapted from [Laurent, 2012](#).

972

973

974 **Supplementary material:**

975 **Table A-** Major and trace element composition of igneous rocks from the Quadrilátero Ferrífero.  
976 Data are from: Gomes, 1985; Carneiro, 1992; Noce et al., 1997; Da Silva et al., 2000; Farina et  
977 al., 2015.



978

979 **Table B.** Summary of U-Pb zircon ages for the basement of the Quadrilátero Ferrífero. Data are  
980 from: Machado and Carneiro, 1992; Machado et al., 1992; Chemale et al., 1993; Noce et al.,  
981 1997; Noce et al., 1998; Romano et al., 2013; Lana et al., 2013; Farina et al., 2015.

982

983 **Table C.** Summary of U-Pb zircon ages for the Rio Das velhas Greenstone Belt. Data are from:  
984 Machado et al., 1992; Machado et al., 1996; Noce et al., 2005; Hartmann et al., 2006.

985

986 **Table D.** Summary of detrital, magmatic and metamorphic ages for the Minas Supergroup.  
987 Data are from: Machado et al., 1992; Babinski et al., 1995; Machado et al., 1996; Brueckner et  
988 al., 2000; Hartmann et al., 2006; Cabral et al., 2012; Koglin et al., 2014; Cassino, 2014; Mendes  
989 et al., 2014.

990

991 **Table E.** Summary of magmatic and metamorphic Rhyacian ages in the Quadrilátero Ferrífero.  
992 Data are from: Belo de Oliveira and Teixeira, 1990; Machado et al., 1992; Babinski et al., 1995;  
993 Schrank & Machado, 1996a; Schrank and Machado, 1996b; Marshak et al., 1997; Noce et al.,  
994 1998.

995

996

997

998

999 **References**

1  
2  
3  
4  
5  
6  
7  
8  
9  
10  
11  
12  
13  
14  
15  
16  
17  
18  
19  
20  
21  
22  
23  
24  
25  
26  
27  
28  
29  
30  
31  
32  
33  
34  
35  
36  
37  
38  
39  
40  
41  
42  
43  
44  
45  
46  
47  
48  
49  
50  
51  
52  
53  
54  
55  
56  
57  
58  
59  
60  
61  
62  
63  
64  
65

- 1  
2  
3  
4  
5  
6  
7  
8  
9  
10  
11  
12  
13  
14  
15  
16  
17  
18  
19  
20  
21  
22  
23  
24  
25  
26  
27  
28  
29  
30  
31  
32  
33  
34  
35  
36  
37  
38  
39  
40  
41  
42  
43  
44  
45  
46  
47  
48  
49  
50  
51  
52  
53  
54  
55  
56  
57  
58  
59  
60  
61  
62  
63  
64  
65
- 1000 Aguilar Gil, C., Farina, F., Lana, C., 2015. Constraining the timing of the Transamazonian  
1001 metamorphic event in the Southern São Francisco Craton (Brazil): revealed by monazite and  
1002 titanite dating. 8<sup>th</sup> Hutton Symposium on Granites and Related Rocks, Florianópolis, Brazil.  
1003  
1004 Albert, C., Farina, F., Lana, C., Gerdes, A., 2015. Archean crustal evolution in the Southern São  
1005 Francisco Craton (Brazil): constraints from U-Pb and Lu-Hf isotope analyses. 8<sup>th</sup> Hutton  
1006 Symposium on Granites and Related Rocks, Florianópolis, Brazil.  
1007  
1008 Alkmim, F.F., Marshak, S., 1998. The Transamazonian orogeny in the Quadrilátero Ferrífero,  
1009 Minas Gerais, Brazil: Paleoproterozoic Collision and Collapse in the Southern São Francisco  
1010 Craton region. *Precambrian Research*, 90, 29–58.  
1011  
1012 Alkmim, F.F. and Noce, C.M. (eds.) 2006. The Paleoproterozoic Record of the São Francisco  
1013 Craton. IGCP 509 Field workshop, Bahia and Minas Gerais, Brazil. Field Guide & Abstracts,  
1014 114 p.  
1015  
1016 Alkmim, F.F., Martins-Neto, M.A., 2012. Proterozoic first-order sedimentary sequences of the  
1017 São Francisco Craton, eastern Brazil. *Marine and Petroleum Geology*, 33, 127–139.  
1018  
1019 Almeida, F.F. M. 1977. O Cráton do São Francisco. *Revista Brasileira de Geociências*, 7, 349-  
1020 364.  
1021

- 1  
2  
3  
4  
5  
6  
7  
8  
9  
10  
11  
12  
13  
14  
15  
16  
17  
18  
19  
20  
21  
22  
23  
24  
25  
26  
27  
28  
29  
30  
31  
32  
33  
34  
35  
36  
37  
38  
39  
40  
41  
42  
43  
44  
45  
46  
47  
48  
49  
50  
51  
52  
53  
54  
55  
56  
57  
58  
59  
60  
61  
62  
63  
64  
65
- 1022 Amorim, L. Q., Alkmim, F. F., 2011. New ore types from the Cauê Banded Iron Formation,  
1023 Quadrilátero Ferrífero, Minas Gerais, Brazil: Responses to the growing demand. In: Iron Ore  
1024 Conference 2011. The Growing Demand. The Australasian Institute of Mining and  
1025 Metallurgy, 2011, p. 59-71.
- 1026
- 1027 Ávila, C.A., Teixeira, W., Cordani, U.G., Moura, C.A.V., Pereira, R.M., 2010. Rhyacian (2.23-2.20)  
1028 juvenile accretion in the southern São Francisco craton, Brazil: Geochemical and isotopic  
1029 evidence from the Serrinha magmatic suite, Mineiro belt. *Journal of South American Earth  
1030 Sciences*, 29, 143-159.
- 1031
- 1032 Babinski, M., Chemale Jr., F., Van Schmus, W.R., 1991. Pb/Pb geochronology of carbonate  
1033 rocks of Minas Supergroup, Quadrilátero Ferrífero, Minas Gerais, Brazil. *Eos, Trans. Am.  
1034 Geophys. Union*, 1991 Fall Meet. Suppl., 72: 531.
- 1035
- 1036 Babinski, M., Chemale Jr, F., Van Schmus, W.R., 1993. A idade das formações ferríferas  
1037 bandadas do Supergrupo Minas e sua correlação com aquelas da África do Sul e Austrália. In:  
1038 Anais II Simposio do Cráton do São Francisco, Salvador, Soc. Bras. Geol., Núcleo Bahia/Sergipe,  
1039 pp. 152–153.
- 1040
- 1041 Babinski, M., Chemale Jr., F., Van Schmus, W.R., 1995. The Pb/Pb age of the Minas Supergroup  
1042 carbonate rocks, Quadrilátero Ferrífero, Brazil. *Precambrian Research*, 72, 235–245.
- 1043

- 1  
2  
3  
4  
5  
6  
7  
8  
9  
10  
11  
12  
13  
14  
15  
16  
17  
18  
19  
20  
21  
22  
23  
24  
25  
26  
27  
28  
29  
30  
31  
32  
33  
34  
35  
36  
37  
38  
39  
40  
41  
42  
43  
44  
45  
46  
47  
48  
49  
50  
51  
52  
53  
54  
55  
56  
57  
58  
59  
60  
61  
62  
63  
64  
65
- 1044 Baltazar, O.F., Zucchetti, M., 2007. Lithofacies associations and structural evolution of the  
1045 Archean Rio das Velhas greenstone belt, Quadrilátero Ferrífero, Brazil: a review of the setting  
1046 of gold deposits. *Ore Geology Reviews* 32, 1–2.
- 1047
- 1048 Barbosa, A.L.M., 1979. Variações de fácies na Série Minas. Bol. Soc. Bras. Geol., Núcleo Minas  
1049 Gerais, 1, 89–100.
- 1050
- 1051 Barbosa, J.S.F., Sabaté, P., 2004. Archean and Paleoproterozoic Crust of the São Francisco  
1052 craton, Bahia, Brazil: geodynamic features. *Precambrian Research*, 133, 1-27.
- 1053
- 1054 Brueckner, H.K., Cunningham, D., Alkmin, F.F., Marshak, S., 2000. Tectonic implications of  
1055 Precambrian Sm–Nd dates from the southern São Francisco craton and adjacent Araçuaí and  
1056 Ribeira belts, Brazil. *Precambrian Research*, 99, 3, 255-269.
- 1057
- 1058 Cabral, A.R., Zeh, A., Koglin, N., Gomes, A.A.S., Viana, D.J., Lehmann, B. 2012. Dating the Itabira  
1059 iron formation, Quadrilátero Ferrífero of Minas Gerais, Brazil, at 2.65 Ga: depositional U–Pb  
1060 age of zircon from a metavolcanic layer. *Precambrian Research*, 204, 40-45.
- 1061
- 1062 Canuto, J.R., 2010. Estratigrafia de seqüências em bacias sedimentares de diferentes idades e  
1063 estilos tectônicos. *Revista Brasileira de Geociências*, 40 (4), 537-549.
- 1064

- 1  
2  
3  
4  
5  
6  
7  
8  
9  
10  
11  
12  
13  
14  
15  
16  
17  
18  
19  
20  
21  
22  
23  
24  
25  
26  
27  
28  
29  
30  
31  
32  
33  
34  
35  
36  
37  
38  
39  
40  
41  
42  
43  
44  
45  
46  
47  
48  
49  
50  
51  
52  
53  
54  
55  
56  
57  
58  
59  
60  
61  
62  
63  
64  
65
- 1065 Carneiro, M.A., 1992a. O Complexo Metamórfico Bonfim Setentrional (Quadrilátero Ferrífero,  
1066 Minas Gerais): Litoestratigrafia e evolução geológica de um segmento de crosta continental do  
1067 Arqueano. Unpublished PhD Thesis, University of São Paulo, Brazil, 233 pp.  
1068  
1069 Carneiro, M.A. 1992b. O Complexo Metamórfico do Bonfim Setentrional. Revista da Escola de  
1070 Minas, 45, 155-156  
1071  
1072 Carneiro, M.A., Teixeira, W., 1992. Discordancia de idades radiometricas U-Pb e Rb-Sr no  
1073 craton do Sao Francisco meridional: evidencias apartir do Complexo Metamórfico Bonfim  
1074 Setentrional, Quadrilátero Ferrífero, Minas Gerais. In: Congresso Brasileiro de Geologia, 37,  
1075 São Paulo, 1992. Resumos. São Paulo, Soc. Bras. Geol., 189-190.  
1076  
1077 Carneiro, M.A., Carvalho Jr., I.M., Teixeira, W., 1998. Petrologia, geoquímica e geocronologia  
1078 dos diques máficos do Complexo Bonfim Setentrional (Quadrilátero Ferrífero) e suas  
1079 implicações na evolução crustal do Cráton São Francisco Meridional. *Revista Brasileira de*  
1080 *Geociências* 28 (1), 29–44.  
1081  
1082 Cassino, L.F., 2014. Distribuição de idades U-Pb de zircões detríticos dos Supergrupos Rio das  
1083 Velhas e Minas na Serra de Ouro Preto, Quadrilátero Ferrífero, MG – Implicações para a  
1084 evolução sedimentar e tectônica. Departamento de Geologia, Universidade Federal de Ouro  
1085 Preto. Thesis, 52p.  
1086

- 1  
2  
3  
4  
5  
6  
7  
8  
9  
10  
11  
12  
13  
14  
15  
16  
17  
18  
19  
20  
21  
22  
23  
24  
25  
26  
27  
28  
29  
30  
31  
32  
33  
34  
35  
36  
37  
38  
39  
40  
41  
42  
43  
44  
45  
46  
47  
48  
49  
50  
51  
52  
53  
54  
55  
56  
57  
58  
59  
60  
61  
62  
63  
64  
65
- 1087 Chauvet, A., Faurre, M., Dossin, I., Charvet, J., 1994. Three-stage structural evolution of the  
1088 Quadrilátero Ferrífero: consequences for Neoproterozoic age and the formation of gold  
1089 concentrations of the Ouro Preto area, Minas Gerais, Brazil. *Precambrian Research*, 68, 139–  
1090 167.  
1091  
1092 Chaves M.L.S.C. 1997. *Geologia e mineralogia do diamante da Serra do Espinhaço em Minas*  
1093 *Gerais*. São Paulo, Tese de Doutorado, IG - Universidade de São Paulo, 289 p.  
1094  
1095 Chemale Jr., F., Rosière, C.A., Endo, I., 1991. Evolução tectônica do Quadrilátero Ferrífero,  
1096 Minas Gerais: um modelo. *Pesquisas* 18(2), 104–127.  
1097  
1098 Chemale Jr, F., Alkmim, F.F., Endo, I 1993. Late Proterozoic tectonism in the interior of the São  
1099 Francisco Craton. *Gondwana Eight-Assembly, Evolution and Dispersal*. Balkema, 29-42.  
1100  
1101  
1102 Chemale Jr., F., Rosière, C.A., Endo, I., 1994. The tectonic evolution of the Quadrilátero  
1103 Ferrífero, Minas Gerais, Brazil. *Precambrian Research*, 65, 25–54.  
1104  
1105 Cordani, U.G., Kawashita, K., Miiller, G., Quade, H., Reimer, V., Roeser, H., 1980. Interpretação  
1106 tectônica e petrológica de dados geocronológicos do embasamento na borda sudeste do  
1107 Quadrilátero Ferrífero. *An. Acad. Bras. Cienc.*, 52: 785-799.  
1108  
1109 Costa, L., Rocha, M.M., de Sousa, R.M., 2003. O ouro do Brasil: transporte e fiscalidade (1720-  
1110 1764). *Anais do V Congresso Brasileiro de História Econômica e 6ª Conferência Internacional*  
1111 *de História de Empresas, Associação Brasileira de Pesquisadores em História Econômica.*

- 1  
2  
3 1112  
4  
5 1113 Dorr II, J.V.N., Gair, J.E., Pomerene, J.G., Ryneanson, G.A., 1957. Revisão da estratigrafia pré-  
6 cambriana do Quadrilátero Ferrífero. DNPM-DFPM, Rio de Janeiro, 31p.  
7  
8 1114  
9  
10 1115  
11 1116 Dorr, J.V.N., II, 1959. Esboço geológico do Quadrilátero Ferrífero de Minas Gerais, Brasil. - Dep.  
12 Nac. Prod. Min., Publ. Espec. 1, Rio de Janeiro.  
13  
14 1117  
15  
16 1118  
17  
18 1119 Dorr II, J.V.N., 1969. Physiographic, Stratigraphic and Structural Development of the  
19 Quadrilátero Ferrífero, Minas Gerais, Brazil. USGS/DNPM, Washington, Prof. Paper 641-A,  
20 1120 110p.  
21  
22 1121  
23  
24 1122  
25  
26 1123 Drake, A.A., Morgan, B.A., 1980. Precambrian plate tectonics in the Brazilian shield; evidence  
27 from the pre-Minas rocks of the Quadrilátero Ferrífero, Minas Gerais. U.S. Geol. Surv. pp. 1–  
28 64. Prof. Paper 1119, U.S. Geological Survey, pp. B1–B19.  
29  
30 1124  
31  
32 1125  
33  
34 1126  
35  
36 1127 Endo, I., Fonseca, M.A., 1992. Sistema de cisalhamento Fundação-Cambotas no Quadrilátero  
37 Ferrífero, MG: Geometria e cinemática. *Rev. da Escola de Minas*, Univ. Federal de Ouro Preto,  
38 Ouro Preto (Brazil ) 45, 28–31.  
39  
40 1128  
41  
42 1129  
43  
44 1130  
45  
46 1131 Endo, I., 1997. Regimes tectônicos do Arqueano e Proterozóico no interior da Placa  
47 Sanfranciscana: Quadrilátero Ferrífero e áreas adjacentes, Minas Gerais. Unpublished PhD  
48 Thesis, University of São Paulo, Brazil, 330p.  
49  
50 1132  
51  
52 1133  
53  
54  
55  
56  
57  
58  
59  
60  
61  
62  
63  
64  
65

- 1  
2  
3 1134  
4  
5 1135 Eriksson, K.A., Krapez, B., Fralick, P.W., 1994. Sedimentology of Archean greenstone belts:  
6 1136 signatures of tectonic evolution. *Earth-Science Reviews*, 37, 1–88.  
7  
8 1137  
9  
10  
11 1138 Farina, F., Albert, C., Lana, C., 2015. The Neoproterozoic transition between medium- and high-K  
12 1139 granitoids: Clues from the Southern São Francisco Craton (Brazil). *Precambrian Research*, 266,  
13 1140 375-394.  
14  
15  
16  
17  
18  
19 1141  
20  
21  
22 1142 Gill, J.B. 1981. *Orogenic Andesites and Plate Tectonics*, 390 pp. Volume 16, Minerals and Rocks.  
23 1143 Berlin, Heidelberg, New York: Springer-Verlag.  
24  
25  
26  
27 1144  
28  
29  
30  
31 1145 Gomes, N.S. 1985. *Petrologisch-geochemische Untersuchungen im Bafao-Komplex Eisernes*  
32 1146 *Viereck, Minas Gerais, Brasilien. Clausthal, 209 pp (Dissertation, Mathematisch-*  
33 1147 *Naturwissenschaftlichen Fakultät, Technische Universität Clausthal).*  
34  
35  
36  
37  
38 1148  
39  
40  
41 1149 Hartmann, L.A., Endo, I., Suita, M.T.F., Santos, J.O.S., Frantz, J.C., Carneiro, M.A., Naughton,  
42 1150 N.J., Barley, M.E., 2006. Provenance and age delimitation of Quadrilátero Ferrífero sandstones  
43 1151 based on zircon U–Pb isotopes. *Journal of South American Earth Sciences*, 20, 273–285.  
44  
45  
46  
47  
48  
49 1152  
50  
51  
52 1153 Herz, N., 1978. *Metamorphic rocks of the Quadrilátero Ferrífero, Minas Gerais, Brazil. United*  
53 1154 *States Geological Survey Professional Paper 641-C. 81 pp.*  
54  
55  
56  
57  
58 1155  
59  
60  
61  
62  
63  
64  
65



- 1  
2  
3  
4  
5  
6  
7  
8  
9  
10  
11  
12  
13  
14  
15  
16  
17  
18  
19  
20  
21  
22  
23  
24  
25  
26  
27  
28  
29  
30  
31  
32  
33  
34  
35  
36  
37  
38  
39  
40  
41  
42  
43  
44  
45  
46  
47  
48  
49  
50  
51  
52  
53  
54  
55  
56  
57  
58  
59  
60  
61  
62  
63  
64  
65
- 1156 Hippertt, J.F., 1994. Structure indicative of helicoidal flow in a migmatitic diapir (Bac\_aõo  
1157 Complex, southeastern Brazil ). *Tectonophysics*, 234, 169–996.
- 1158
- 1159 Hippertt, J.F., Borba, R.P., Nalini, H.A., 1992. O contato Formac\_ão Moeda-Complexo do  
1160 Bonfim: Uma zona de cislhamento normal na borda oeste do Quadrilátero Ferrífero, MG.  
1161 *Rev. da Escola de Minas, Univ. Federal de Ouro Preto*, 45, 32–34.
- 1162
- 1163 Jordt-Evangelista, H., Alkmim, F.F., Marshak, S., 1992. Metamorfismo progressivo e a  
1164 ocorrência dos 3 polimorfos  $Al_2SiO_5$  (cianita, andaluzita e sillimanita) na Formação Sabará em  
1165 Ibirité, Quadrilátero Ferrífero, MG. *Rev. Da Escola de Minas, Univ. Federal de Ouro Preto, Ouro*  
1166 *Preto (Brazil)* 45, 157–160.
- 1167
- 1168 Klein, C., Ladeira, E.A., 2000. Geochemistry and petrology of some Proterozoic banded iron-  
1169 formations of the Quadrilátero Ferrífero, Minas Gerais, Brazil. *Economic Geology*, 95 (2), 405-  
1170 427.
- 1171
- 1172 Koglin, N., Cabral, A.R., Brunetto, W.J., Vymazalová, A., 2012. Gold–tourmaline assemblage in a  
1173 Witwaterstrand-like gold deposit, Ouro Fino, Quadrilátero Ferrífero of Minas Gerais, Brazil: the  
1174 composition of gold and metallogenic implications. *Neues Jahrbuch für Mineralogie-*  
1175 *Abhandlungen: Journal of Mineralogy and Geochemistry*, 189 (3), 263-273.
- 1176
- 1177 Koglin, N., Zeh, A., Cabral, A.R., Gomes, A.A.S., Neto, A.V.C., Brunetto, W.J., Galbiatti, H., 2014.  
1178 Depositional age and sediment source of the auriferous Moeda Formation, Quadrilátero  
1179 Ferrífero of Minas Gerais, Brazil: New constraints from U–Pb–Hf isotopes in zircon and  
1180 xenotime. *Precambrian Research*, 255, 96-108.

- 1181
- 1  
2 1182 Ladeira, E.A., Roeser, H.M.P., Tobschal, H.J., 1983. Evolução petrogenética do Cinturão de  
3  
4 1183 Rochas Verdes, Rio das Velhas, Quadrilátero Ferrífero, Minas Gerais. 2<sup>th</sup> Simpósio de Geologia  
5  
6  
7 1184 de Minas Gerais. Sociedade Brasileira de Geologia, Belo Horizonte, pp. 149–165.  
8  
9 1185
- 10  
11 1186 Lana, C., Alkmim, F.F., Armstrong, R., Scholz, R., Romano, R., Nalini, H.A., 2013. The ancestry  
12  
13 1187 and magmatic evolution of Archaean TTG rocks of the Quadrilátero Ferrífero province,  
14  
15 1188 southeast Brazil. *Precambrian Research*, 231, 157-173.  
16  
17  
18 1189
- 19  
20  
21 1190 Laurent, O., Martin, H., Moyen, J.F., Doucelance, 2014. The diversity and evolution of late-  
22  
23 1191 Archean granitoids: Evidence for the onset of “modern-style” plate tectonic between 3.0 and  
24  
25 1192 2.5 Ga.. *Lithos*, 205, 208-235.  
26  
27  
28 1193
- 29  
30 1194 Lobato, L.M., Ribeiro-Rodrigues, L.C., Vieira, F.W.R., 2001. Brazil's premier gold province: Part  
31  
32 1195 II. Geology and genesis of gold deposits in the Archean Rio das Velhas greenstone belt,  
33  
34 1196 Quadrilátero Ferrífero. *Mineralium Deposita*, 36, 249–277.  
35  
36  
37 1197
- 38  
39 1198 McDonough, W.F., Sun, S.S. 1995. The composition of the Earth. *Chemical Geology*, 120 (3),  
40  
41 1199 223-253.  
42  
43  
44 1200
- 45  
46 1201 Machado, N., Carneiro, M.A., 1992. U-Pb evidence of Late Archean tectonothermal activity in  
47  
48 1202 southern São Francisco shield, Brazil. *Canadian Journal of Earth Sciences*, 29, 2341–2346.  
49  
50  
51 1203
- 52  
53  
54  
55  
56  
57  
58  
59  
60  
61  
62  
63  
64  
65

- 1  
2  
3  
4  
5  
6  
7  
8  
9  
10  
11  
12  
13  
14  
15  
16  
17  
18  
19  
20  
21  
22  
23  
24  
25  
26  
27  
28  
29  
30  
31  
32  
33  
34  
35  
36  
37  
38  
39  
40  
41  
42  
43  
44  
45  
46  
47  
48  
49  
50  
51  
52  
53  
54  
55  
56  
57  
58  
59  
60  
61  
62  
63  
64  
65
- 1204 Machado, N., Noce, C.M., Ladeira, E.A., de Oliveira, O.A.B., 1992. U-Pb geochronology of the  
1205 Archean magmatism and Proterozoic metamorphism in the Quadrilátero Ferrífero, southern  
1206 São Francisco Craton, Brazil. *Geological Society of America Bulletin*, 104, 1221–1227.  
1207  
1208 Machado, N., Schrank, A., Noce, C.M., Gauthier, G., 1996. Ages of detrital zircon from Archean-  
1209 Paleoproterozoic sequences: Implications for Greenstone Belt setting evolution of a  
1210 Transamazonian foreland basin in Quadrilátero Ferrífero, southeast Brazil. *Earth and Planetary  
1211 Science Letters*, 141, 259–276.  
1212  
1213 Machado, M.M.M., 2009. Construindo a imagem geológica do Quadrilátero Ferrífero:  
1214 conceitos e representações. Universidade Federal de Minas Gerais, Belo Horizonte, Brasil.  
1215 Master Thesis, 296 pp.  
1216  
1217 Marshak, S., Alkmim, F.F., Jordt-Evangelista, H., 1992. Proterozoic crustal extension and the  
1218 generation of dome-and-keel structures in an Archaean granite–greenstone terrane. *Nature*  
1219 357, 491–493.  
1220  
1221 Marshak, S., Tinkham, D., Alkmim, F.F., Brueckner, H., 1997. Dome-and-keel provinces formed  
1222 during Paleoproterozoic orogenic collapse- Diapir clusters or core complexes? Examples from  
1223 the Quadrilátero Ferrífero (Brazil ) and the Penokean Orogen (USA). *Geology*, 25, 415-418.  
1224

- 1  
2  
3  
4  
5  
6  
7  
8  
9  
10  
11  
12  
13  
14  
15  
16  
17  
18  
19  
20  
21  
22  
23  
24  
25  
26  
27  
28  
29  
30  
31  
32  
33  
34  
35  
36  
37  
38  
39  
40  
41  
42  
43  
44  
45  
46  
47  
48  
49  
50  
51  
52  
53  
54  
55  
56  
57  
58  
59  
60  
61  
62  
63  
64  
65
- 1225 Martin, H., Moyen, J.F., Rapp, R., 2009. The sanukitoid series: magmatism at the Archaean–  
1226 Proterozoic transition. *Earth and Environmental Science Transactions of the Royal Society of*  
1227 *Edinburgh*, 100 (1-2), 15-33.
- 1228
- 1229 Maxwell, C. H., 1958. The Batatal Formation: Soc. Bras. Geol. Bol., 7, 2, 60-61.
- 1230
- 1231 Mendes, M.D.C.O., Lobato, L.M., Suckau, V., Lana, C., 2014. Datação U-Pb in situ por LA-ICPMS  
1232 em zircões detríticos da Formação Cercadinho, Supergrupo Minas. *Geologia USP. Série*  
1233 *Científica*, 14 (1), 55-68.
- 1234
- 1235 Moraes M.A.S. 1985. Reconhecimento de facies sedimentares em rochas metamórficas da  
1236 região de Outro Preto (MG). *In: Soc. Bras. Geol. Simp. Geol. Minas Gerais*, 3, Belo Horizonte,  
1237 5:84-93.
- 1238
- 1239 Moreira, H., Lana, C., 2015. The Hf features of the southern São Francisco Craton basement: a  
1240 detrital zircon record view. 8<sup>th</sup> Hutton Symposium on Granites and Related Rocks,  
1241 Florianópolis, Brazil.
- 1242
- 1243 Moyen, J.F., 2011. The composite Archaean grey gneisses: petrological significance, and  
1244 evidence for a non-unique tectonic setting for Archaean crustal growth. *Lithos*, 123(1), 21-36.
- 1245
- 1246 Moyen, J. F., & Martin, H., 2012. Forty years of TTG research. *Lithos*, 148, 312-336.

- 1247
- 1  
2
- 3 1248 Noce, C.M., 1995. Geocronologia dos eventos magmáticos, sedimentares e metamórficos na  
4  
5 1249 região do Quadrilátero Ferrífero, Minas Gerais. PhD Theses, University of São Paulo, Brazil, 129  
6  
7 1250 pp.  
8  
9  
10 1251  
11  
12  
13 1252 Noce, C. M., Teixeira, W., Machado, N., 1997. Geoquímica dos gnaisses TTG e granitóides  
14  
15 1253 neoarqueanos do Complexo Belo Horizonte, Quadrilátero Ferrífero, Minas Gerais. *Brazilian*  
16  
17 1254 *Journal of Geology*, 27 (1), 25-32.  
18  
19  
20  
21 1255  
22  
23  
24 1256 Noce, C.M., Machado, N., Teixeira, W., 1998. U-Pb geochronology of gneisses and granitoids in  
25  
26 1257 the Quadrilátero Ferrífero (Southern São Francisco Craton): age constraints for Archean and  
27  
28 1258 Paleoproterozoic magmatism and metamorphism. *Revista Brasileira de Geociências*, 28, 95–  
29  
30 1259 102.  
31  
32  
33  
34 1260  
35  
36  
37 1261 Noce, C.M., Zucchetti, M., Baltazar, O.F., Armstrong, R., Dantas, E.L., Renger, F.E., Lobato, L.M.,  
38  
39 1262 2005. Age of felsic volcanism and the role of ancient continental crust in the evolution of the  
40  
41 1263 Neoproterozoic Rio das Velhas greenstone belt (Quadrilátero Ferrífero, Brazil): U–Pb zircon dating  
42  
43 1264 of volcanoclastic graywackes. *Precambrian Research*, 141, 67–82.  
44  
45  
46  
47 1265  
48  
49  
50 1266 Noce, C.M., Pedrosa-Soares, A.C., Silva, L.C., Armstrong, R., Piuzana, D., 2007. Evolution of  
51  
52 1267 polycyclic basement in the Araçuaí Orogen based on U-Pb SHRIMP data: implications for the  
53  
54 1268 Brazil-Africa links in the Paleoproterozoic time. *Precambrian Research*, 159, 60–78.  
55  
56  
57  
58 1269  
59  
60  
61  
62  
63  
64  
65

- 1  
2  
3  
4  
5  
6  
7  
8  
9  
10  
11  
12  
13  
14  
15  
16  
17  
18  
19  
20  
21  
22  
23  
24  
25  
26  
27  
28  
29  
30  
31  
32  
33  
34  
35  
36  
37  
38  
39  
40  
41  
42  
43  
44  
45  
46  
47  
48  
49  
50  
51  
52  
53  
54  
55  
56  
57  
58  
59  
60  
61  
62  
63  
64  
65
- 1270 De Oliveira, O.B., Teixeira, W., 1990. Evidências de uma tectônica tangencial proterozóica no  
1271 Quadrilátero Ferrífero, MG. *Anais 36<sup>th</sup> Congr. Bras. Geol.*, 6, 2589-2604.  
1272  
1273 Oliveira, E.P., Souza, Z.S., Gomes, L.C.C., 2008. U-Pb dating of deformed mafic dyke and host  
1274 gneiss: implications for understanding reworking processes on the western margin of the  
1275 Archaean Uauá block, Ne São Francisco Craton, Brazil. *Brazilian Journal of Geology*, 30 (1), 149-  
1276 152.  
1277  
1278 O'Rourke, J.E., 1957. The stratigraphy of metamorphic rocks of the Rio de Pedras and  
1279 Gandarela quadrangles, Minas Gerais, Brazil. PhD thesis, University of Winscosin. Winscosin,  
1280 106 pp.  
1281  
1282 Pedrosa-Soares, A.C., Noce, C.M., Wiedemann, C.M., Pinto, C.P., 2001. The Araçuaí-West  
1283 Congo orogen in Brazil: An overview of a confined orogen formed during Gondwanland  
1284 assembly. *Precambrian Research*, 110, 307–323.  
1285  
1286 Percival, J.A., McNicoll, V., Bailes, A.H., 2006. Strike-slip juxtaposition of ca. 2.72 Ga juvenile arc  
1287 and >2.98 Ga continent margin sequences and its implications for Archean terrane accretion,  
1288 western Superior Province, Canada. *Canadian Journal of Earth Sciences*, 43 (7), 895-927.  
1289  
1290 Pimentel, M.M., Rodrigues, J.B., DellaGiustina, M.E.S., Junges, S., Matteini, M., Armstrong, R.,  
1291 2011. The tectonic evolution of the Neoproterozoic Brasília Belt, central Brazil, based on

- 1  
2  
3  
4  
5  
6  
7  
8  
9  
10  
11  
12  
13  
14  
15  
16  
17  
18  
19  
20  
21  
22  
23  
24  
25  
26  
27  
28  
29  
30  
31  
32  
33  
34  
35  
36  
37  
38  
39  
40  
41  
42  
43  
44  
45  
46  
47  
48  
49  
50  
51  
52  
53  
54  
55  
56  
57  
58  
59  
60  
61  
62  
63  
64  
65
- 1292 SHRIMP and LA-ICPMS UePb sedimentary provenance data: a review. *Journal of South America*  
1293 *Earth Sciences*, 31, 345-357.  
1294  
1295 Pires, F.R.M., 1979. Structural geology and stratigraphy at the junction of the Serra do Curral  
1296 anticline and the Moeda syncline, Quadrilátero Ferrífero, Minas Gerais, Brazil. Ph.D. Thesis,  
1297 University of Michigan, Ann Arbor, U.S.A.  
1298  
1299 Pires, F.R.M., Aranha, D.M., Cabral, A.R., 2005. Volcanic Origin of the Proterozoic Itabira Iron  
1300 Formation, Quadrilátero Ferrífero, Minas Gerais, Brazil, in Proceedings Iron Ore 2005, pp 119-  
1301 121 (The Australasian Institute of Mining and Metallurgy: Melbourne).  
1302  
1303 Pomerene, J.B., 1964. The geology and ore deposits of the Belo Horizonte, Ibirité and Macacos  
1304 quadrangles, Minas Gerais, Brazil. U.S. Geology Survey Prof Paper 341-D, U.S. Geology Survey,  
1305 U.S.A.  
1306  
1307 Reis, L.A., Martins-Neto, M.A., Gomes, N.S., Endo, I., 2002. A bacia de antepaís  
1308 paleoproterozóica Sabará, Quadrilátero Ferrífero, MG. *Revista Brasileira de Geociências*, 32, 43-  
1309 58.  
1310  
1311 Renger, F.E., Silva, R.M.P., Suckau, V.E., 1988. Ouro nos conglomerados da Formação Moeda,  
1312 Sinclinal de Gandarela, Quadrilátero Ferrífero, Minas Gerais. Congr. Bras. Geol, Soc. Bras. Geol.  
1313 35, 44-57.  
1314

- 1  
2  
3  
4  
5  
6  
7  
8  
9  
10  
11  
12  
13  
14  
15  
16  
17  
18  
19  
20  
21  
22  
23  
24  
25  
26  
27  
28  
29  
30  
31  
32  
33  
34  
35  
36  
37  
38  
39  
40  
41  
42  
43  
44  
45  
46  
47  
48  
49  
50  
51  
52  
53  
54  
55  
56  
57  
58  
59  
60  
61  
62  
63  
64  
65
- 1315 Renger, F.E., Noce, C.M., Romano, A.W., Machado, N., 1995. Evolução sedimentar do  
1316 Supergrupo Minas: 500 Ma de registro geológico no Quadrilátero Ferrífero, Minas Gerais,  
1317 Brasil. *Geonomos* 2 (1), 1–11.  
1318  
1319 Rogers, J.J., 1996. A history of continents in the past three billion years. *The Journal of Geology*,  
1320 91-107.  
1321  
1322 Rogers, J.J., and Santosh, M., 2004. *Continents and supercontinents*. Oxford University Press.  
1323  
1324 Romano, R., Lana, C., Alkmim, F.F., Stevens, G.S., Armstrong, R., 2013. Stabilization of the  
1325 southern portion of the São Francisco Craton, SE Brazil, through a long-lived period of potassic  
1326 magmatism. *Precambrian Research*, 224, 143–159.  
1327  
1328 Rosière, C A and Chemale Jr, F, 2006. Itabiritos e minérios de ferro de alto teor do Quadrilátero  
1329 Ferrífero – Uma visão geral e discussão. *Geonomos*, 8, 27-43.  
1330  
1331 Rosière, C.A., Spier, C.A., Rios, F.J., Suckau, V.E., 2008. The itabirites of the Quadrilátero  
1332 Ferrífero and related high-grade iron ore deposits: an overview. *Reviews in Economic Geology*  
1333 15, 223–254.  
1334



1  
2  
3  
4  
5  
6  
7  
8  
9  
10  
11  
12  
13  
14  
15  
16  
17  
18  
19  
20  
21  
22  
23  
24  
25  
26  
27  
28  
29  
30  
31  
32  
33  
34  
35  
36  
37  
38  
39  
40  
41  
42  
43  
44  
45  
46  
47  
48  
49  
50  
51  
52  
53  
54  
55  
56  
57  
58  
59  
60  
61  
62  
63  
64  
65

1335 Sandiford, M., McLaren, S., 2002. Tectonic feedback and the ordering of heat producing  
1336 elements within the continental lithosphere. *Earth and Planetary Science Letters*, 204 (1), 133-  
1337 150.  
1338  
1339 Seixas, L.A.R., David, J., Stevenson, R., 2012. Geochemistry, Nd isotopes and U–Pb  
1340 geochronology of a 2350 Ma TTG suite, Minas Gerais, Brazil: implications for the crustal  
1341 evolution of the southern São Francisco craton. *Precambrian Research*, 196, 61–80.  
1342  
1343 Seixas, L. A. R., Bardintzeff, J. M., Stevenson, R., Bonin, B., 2013. Petrology of the high-Mg  
1344 tonalites and dioritic enclaves of the ca. 2130Ma Alto Maranhão suite: Evidence for a major  
1345 juvenile crustal addition event during the Rhyacian orogenesis, Mineiro Belt, southeast Brazil.  
1346 *Precambrian Research*, 238, 18-41.  
1347  
1348 Simmons, G.C., 1968. Geology and iron deposits of the western Serra do Curral, Minas Gerais,  
1349 Brazil: U.S. Geol. Survey. Paper 341-G, 57 p.968.  
1350  
1351 Simmons, G.C., Maxwell, C.H., 1961, Grupo Tamanduá da Serie Rio das Velhas: Brazil Dept.  
1352 Nac. Produção Mineral, Div. Geologia e Mineralogia, Bol. 211, 30.  
1353  
1354 Schorscher, H.D., 1978. Komatiíitos na estrutura “Greenstone Belt” Série Rio das Velhas,  
1355 Quadrilátero Ferrífero, Minas Gerais, Brasil. 30<sup>th</sup> Congr. Bras. Geol., Recife. Soc. Bras. Geol.,  
1356 292–293.  
1357

- 1358
- 1  
2
- 3 1359 Schrank, A., Machado, N., 1996a. Idades U–Pb em monazitas e zircões das Minas de Morro  
4  
5 1360 Velho e Passagem de Mariana, Quadrilátero Ferrífero, MG. In: Anais 39<sup>th</sup> Congr. Bras. Geol.,  
6  
7 1361 Salvador. Soc. Bras. Geol., 6, 470-472.  
8  
9
- 10 1362
- 11  
12
- 13 1363 Schrank, A., Machado, N., 1996b. Idades U–Pb em monazitas e zircões do distrito aurífero de  
14  
15 1364 Caeté, da Mina de Cuiabá e do Depósito de Carrapato, Quadrilátero Ferrífero (MG). In: Anais  
16  
17 1365 39<sup>th</sup> Congr. Bras. Geol., Salvador. Soc. Bras. Geol., 6, 473-475.  
18  
19  
20
- 21 1366
- 22  
23
- 24 1367 Sichel, S.E., 1983. Geologia das rochas Pré-Cambrianas da região de Barão de Cocais e  
25  
26 1368 geoquímica preliminar dos komatiitos do Supergrupo Rio das Velhas, Quadrilátero Ferrífero,  
27  
28 1369 MG. MSc thesis, Departamento de Geologia, Universidade Federal do Rio de Janeiro. Rio de  
29  
30 1370 Janeiro, Brasil, 232 pp.  
31  
32  
33
- 34 1371
- 35  
36
- 37 1372 Silva, L.C., Noce, C.M., Lobato, L.M., 2000. Dacitic volcanism in the course of the Rio das Velhas  
38  
39 1373 (2800–2960 Ma) Orogeny: a Brazilian Archean analogue (TTD) to the modern adakites. *Revista*  
40  
41 1374 *Brasileira de Geociências*, 30, 384–387.  
42  
43  
44
- 45 1375
- 46  
47
- 48 1376 Souza, P.C., Miller, G., 1984. Primeiras estruturas algais comprovadas na Formação Gandarela,  
49  
50 1377 Quadrilátero Ferrífero. *Revista de Escola de Minas, Ouro Preto*, 2, 161-198.  
51  
52  
53
- 54 1378
- 55  
56
- 57 1379 Teixeira, W., Figueiredo, M.C.H., 1991. An outline of Early Proterozoic crustal evolution in the  
58  
59 1380 São Francisco Craton. Brazil: a review. *Precambrian Research*, 53, 1–22.  
60  
61  
62  
63  
64  
65

- 1  
2  
3 1381  
4  
5 1382 Teixeira, W., Carneiro, M.A., Noce, C.A., Machado, N., Sato, K., Taylor, P.N., 1996. Pb, Sr and Nd  
6  
7 1383 isotope constraints on the Archean evolution of gneissic granitoid complexes in the southern  
8  
9 1384 São Francisco Craton, Brazil. *Precambrian Research*, 78, 151–164.  
10  
11 1385  
12  
13 1386 Teixeira, W., Sabaté, P., Barbosa, J., Noce, C.M., Carneiro, M.A., 2000. Archean and  
14  
15 1387 Paleoproterozoic tectonic evolution of the São Francisco Craton, Brazil. In: Cordani, U.G., Milani,  
16  
17 1388 E.J., Thomaz F., A., Campos, D.A. (Eds.), *Tectonic Evolution of South América*. Rio de Janeiro,  
18  
19 1389 31<sup>st</sup> International Geological Congress. Rio de Janeiro, 101–137.  
20  
21  
22  
23  
24 1390  
25  
26  
27 1391 Teixeira, W., Ávila, C.A., Nunes, L.C., 2008. Nd–Sr isotopic geochemistry and U–Pb  
28  
29 1392 geochronology of the Fé Granite Gneiss and Lajedo Granodiorite: implications for the  
30  
31 1393 Paleoproterozoic Evolution of the Mineiro belt, southern São FranciscoCraton, Brazil. *Revista*  
32  
33 1394 *do Instituto de Geociências-USP, Série Científica* 8, 53–74.  
34  
35  
36  
37 1395  
38  
39  
40 1396 Teixeira, W., Ávila, C.A., Dussin, I.A., Neto, A.C., Bongioiolo, E.M., Santos, J.O., Barbosa, N.S.,  
41  
42 1397 2015. A juvenile accretion episode (2.35–2.32 Ga) in the Mineiro belt and its role to the Minas  
43  
44 1398 accretionary orogeny: Zircon U–Pb–Hf and geochemical evidences. *Precambrian Research*, 256,  
45  
46 1399 148-169.  
47  
48  
49  
50 1400  
51  
52  
53 1401 Villaça J.N. 1981. Alguns aspectos sedimentares da Formação Moeda. *Sociedade Brasileira de*  
54  
55 1402 *Geologia, Núcleo MG*, 2, 92-137.  
56  
57  
58  
59 1403  
60  
61  
62  
63  
64  
65

1  
2  
3  
4  
5  
6  
7  
8  
9  
10  
11  
12  
13  
14  
15  
16  
17  
18  
19  
20  
21  
22  
23  
24  
25  
26  
27  
28  
29  
30  
31  
32  
33  
34  
35  
36  
37  
38  
39  
40  
41  
42  
43  
44  
45  
46  
47  
48  
49  
50  
51  
52  
53  
54  
55  
56  
57  
58  
59  
60  
61  
62  
63  
64  
65

1404 Zhao, G., Sun, M., Wilde, S.A., Li, S., 2004. A Paleo-Mesoproterozoic supercontinent: assembly,  
1405 growth and breakup. *Earth-Science Reviews*, 67 (1), 91-123.  
1406  
1407 Wallace, R.M., 1965. Geology and mineral resources of the Pico de Itabirito district, Minas  
1408 Gerais, Brazil: U.S. Geol. Survey Prof. Paper 341-F, 68 p.  
1409  
1410 Watkins, J.M., Clemens, J.D., Treloar, P.J., 2007. Archaean TTGs as sources of younger granitic  
1411 magmas: melting of sodic metatonalites at 0.6–1.2 GPa. *Contributions to Mineralogy and*  
1412 *Petrology*, 154 (1), 91-110.  
1413  
1414 Zucchetti, M., Lobato, L.M., Baltazar, O.F., 2000. Volcanic and volcanoclastic features in Archaean  
1415 rocks and their tectonic environment, Rio das Velhas Greenstone Belt, Quadrilátero Ferrífero,  
1416 MG, Brazil. *Revista Brasileira de Geociências* 30, 388–392.  
1417

Figure 1  
[Click here to download high resolution image](#)

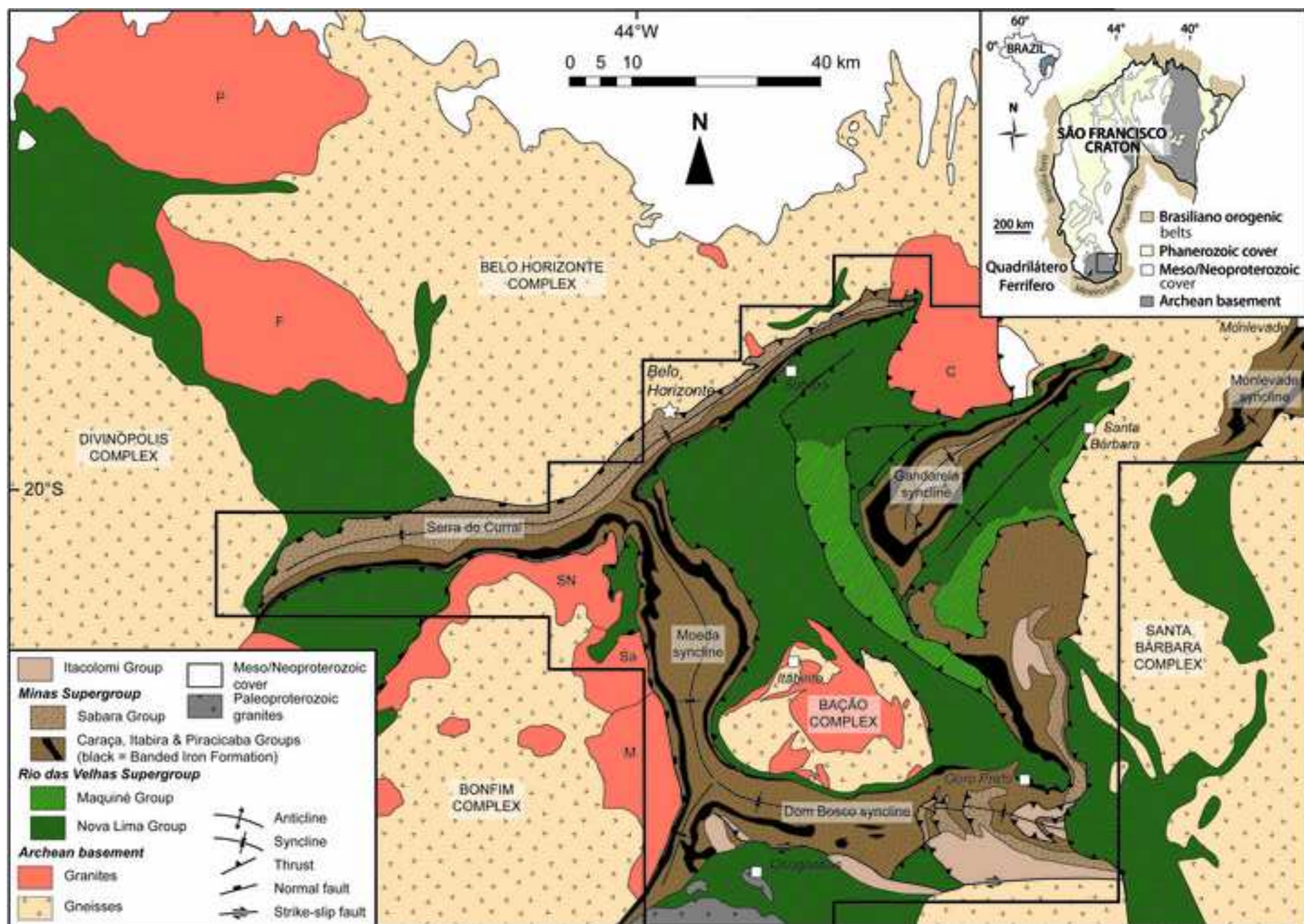


Figure 2  
[Click here to download high resolution image](#)

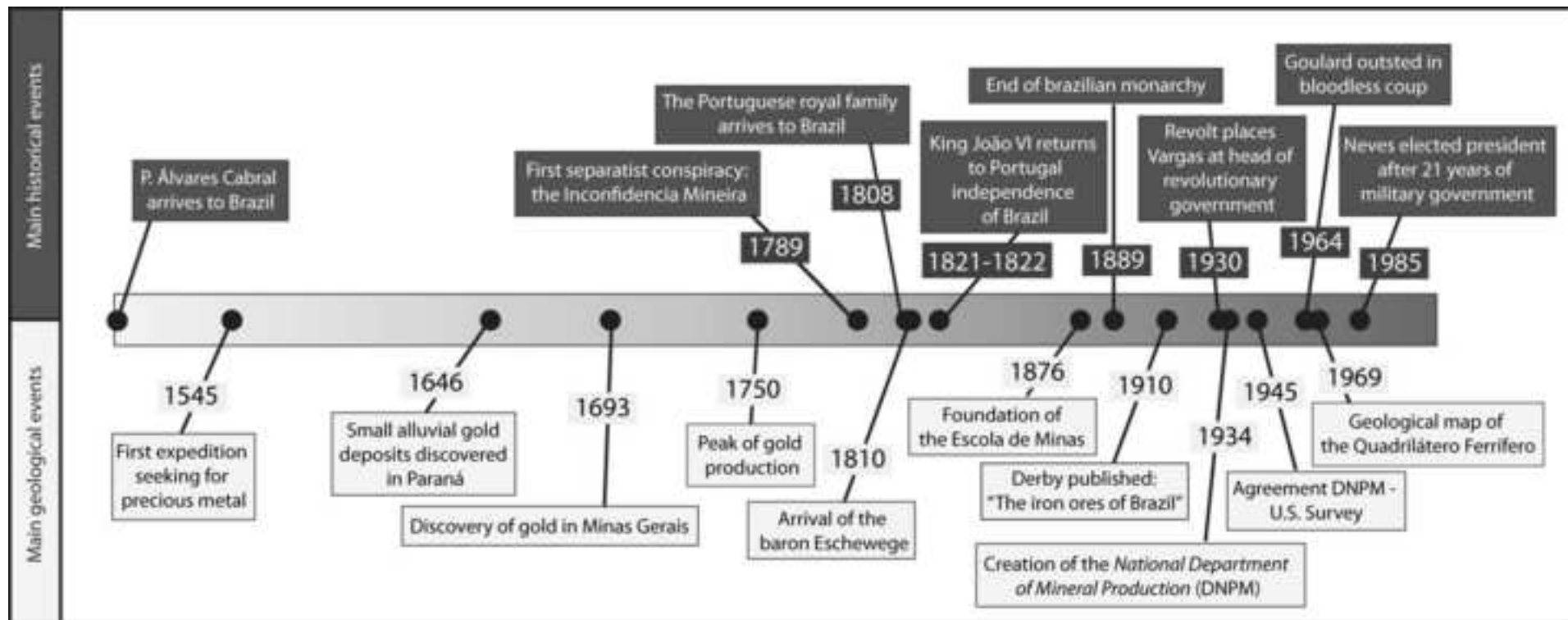




Figure 3  
[Click here to download high resolution image](#)

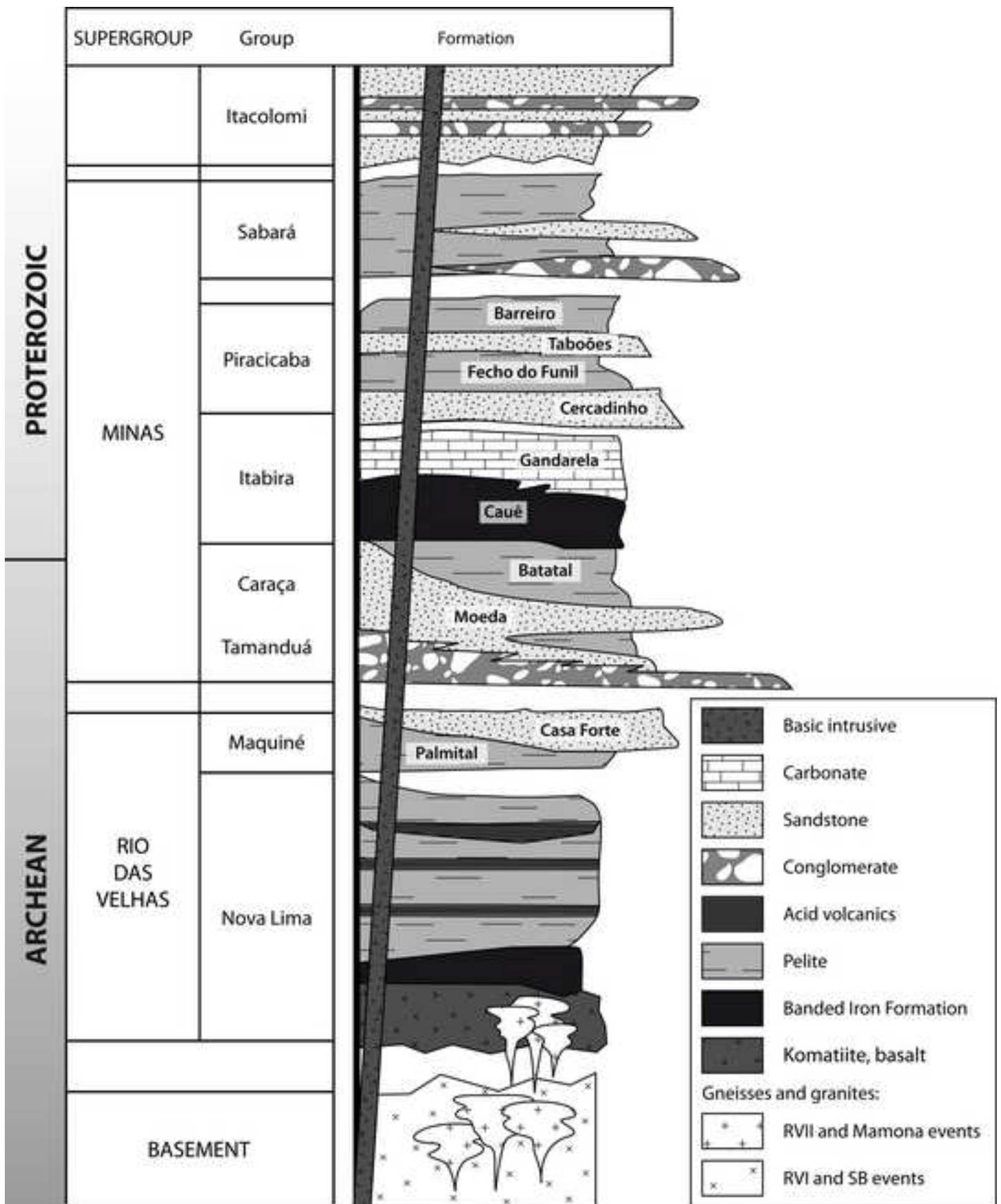


Figure 4  
[Click here to download high resolution image](#)

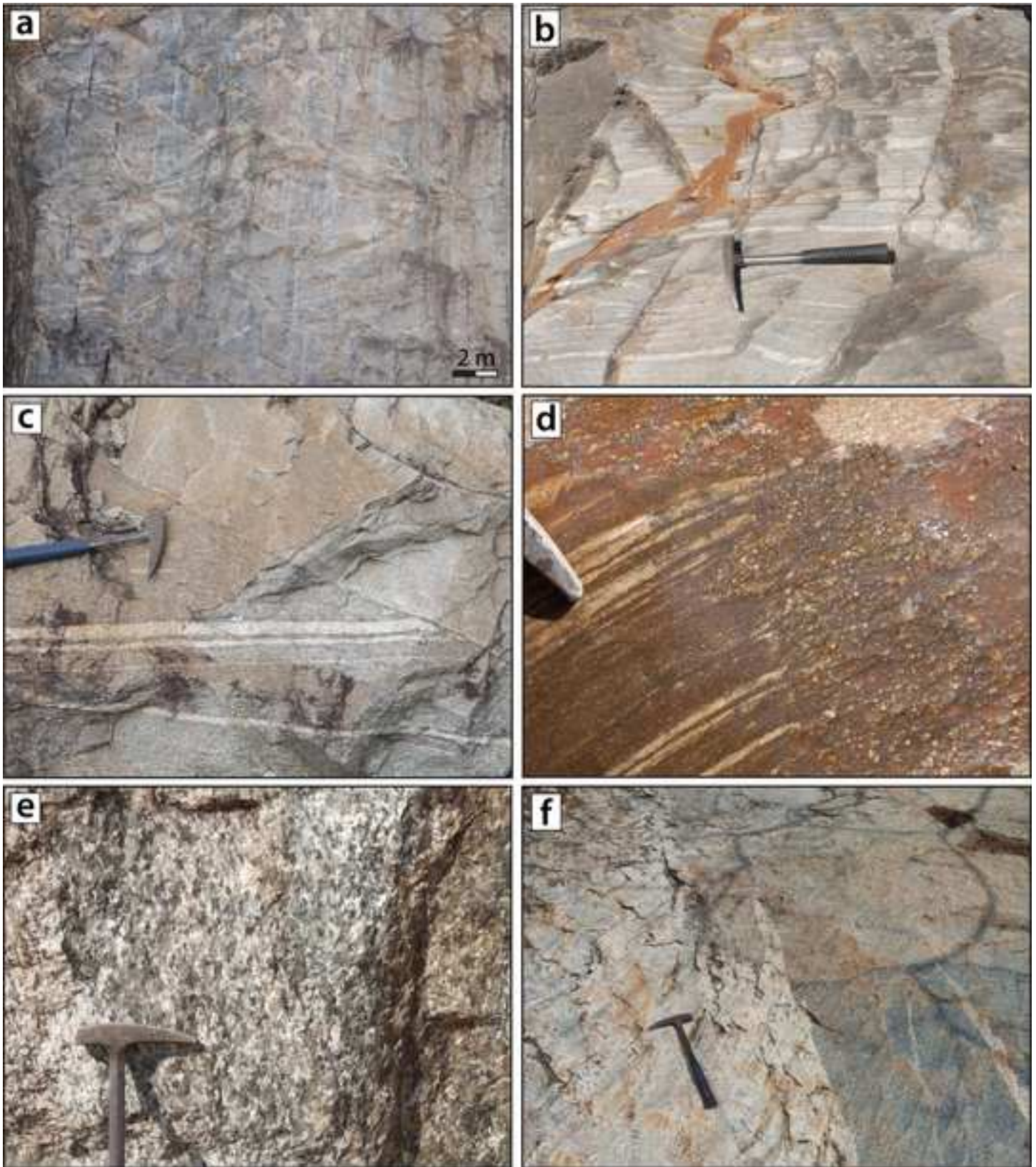




Figure 5  
[Click here to download high resolution image](#)

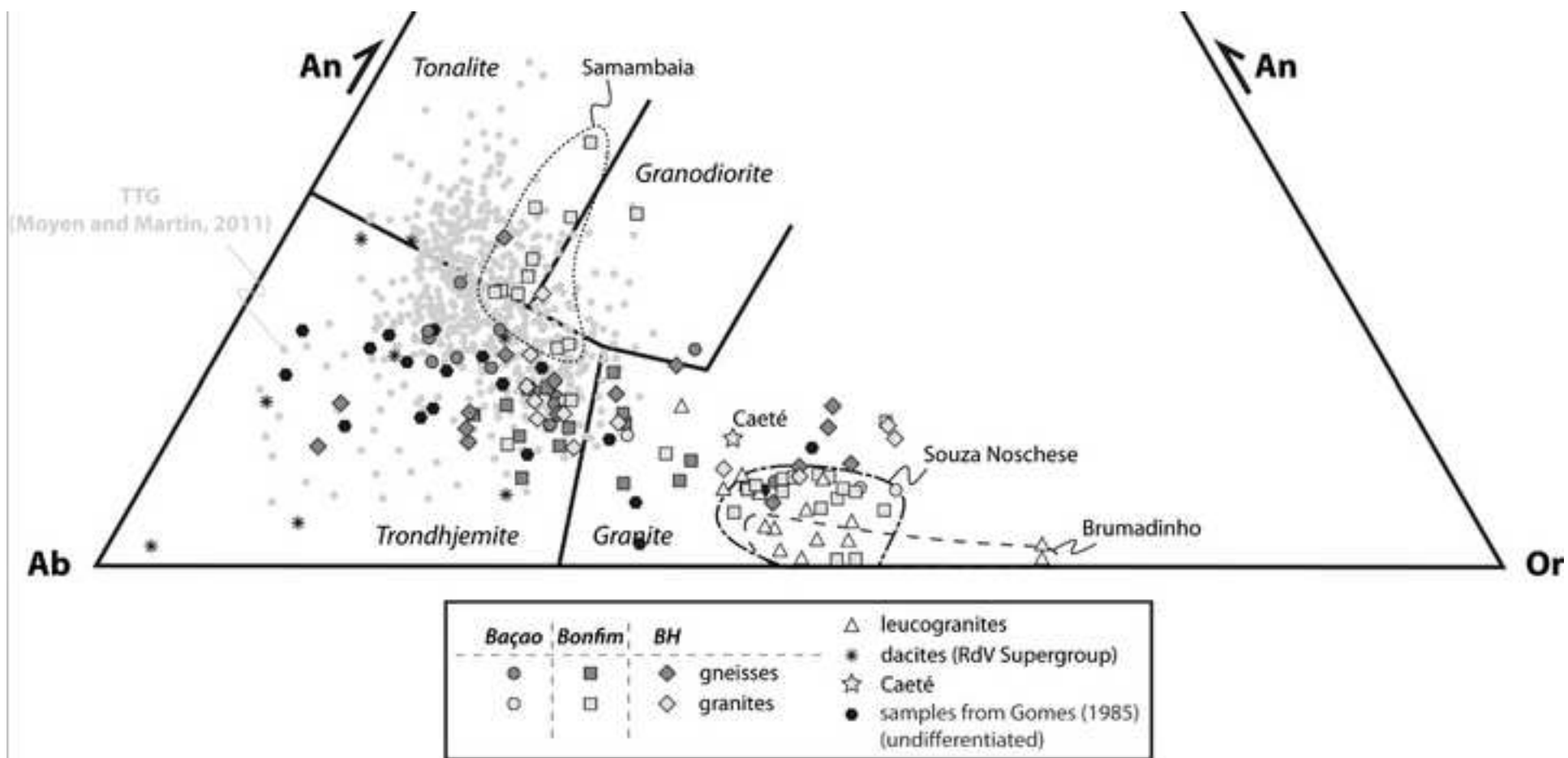


Figure 6  
[Click here to download high resolution image](#)

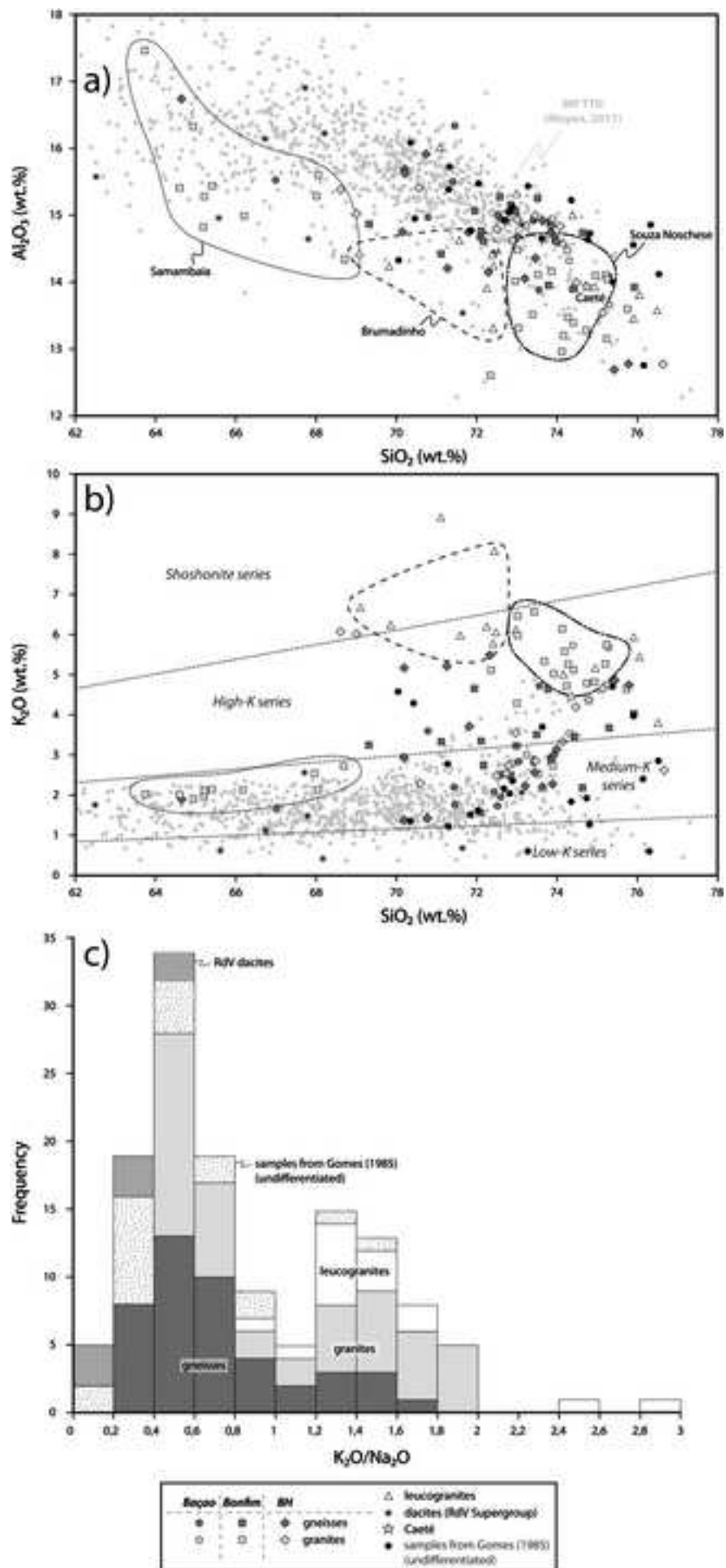


Figure 7  
[Click here to download high resolution image](#)

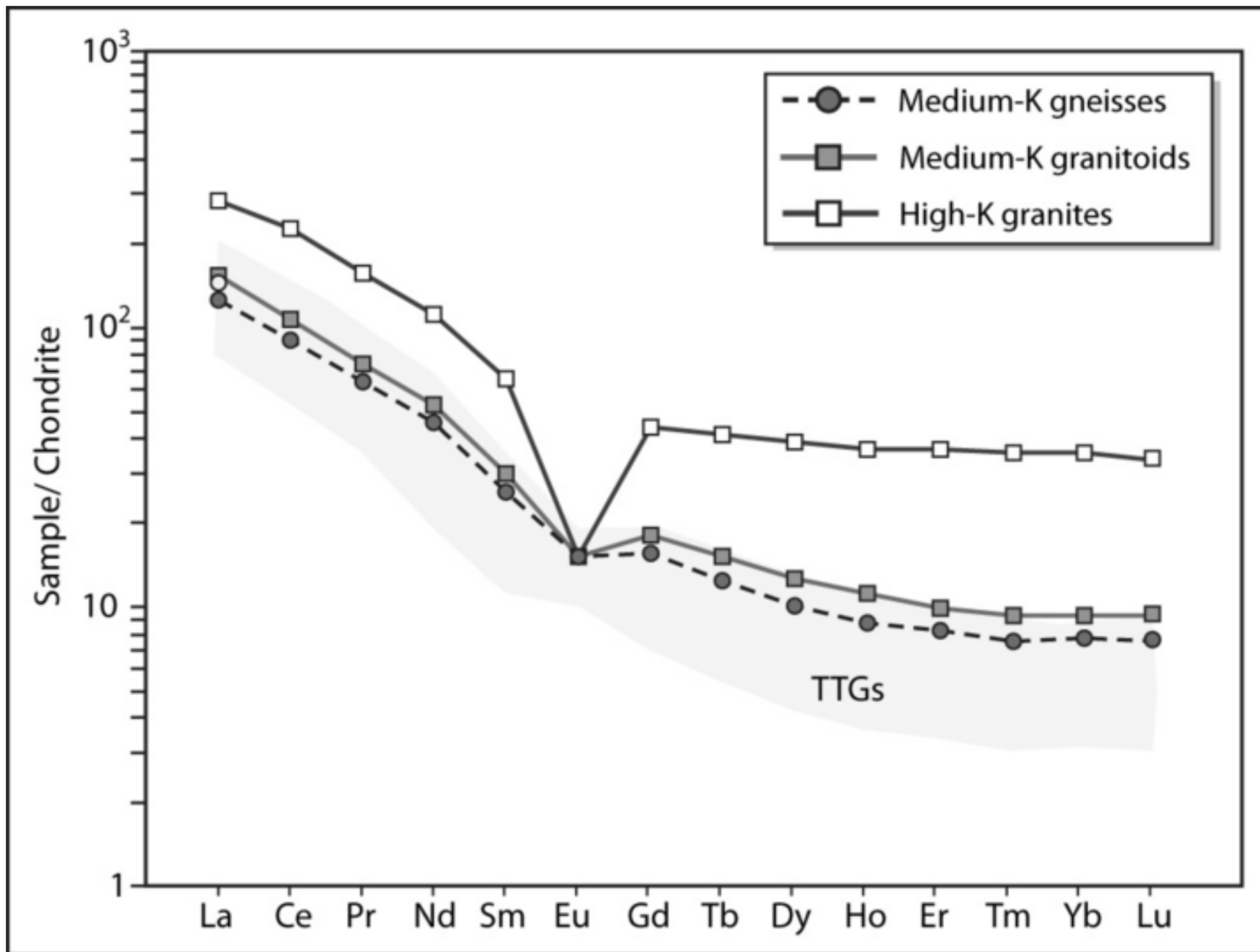


Figure 8  
[Click here to download high resolution image](#)

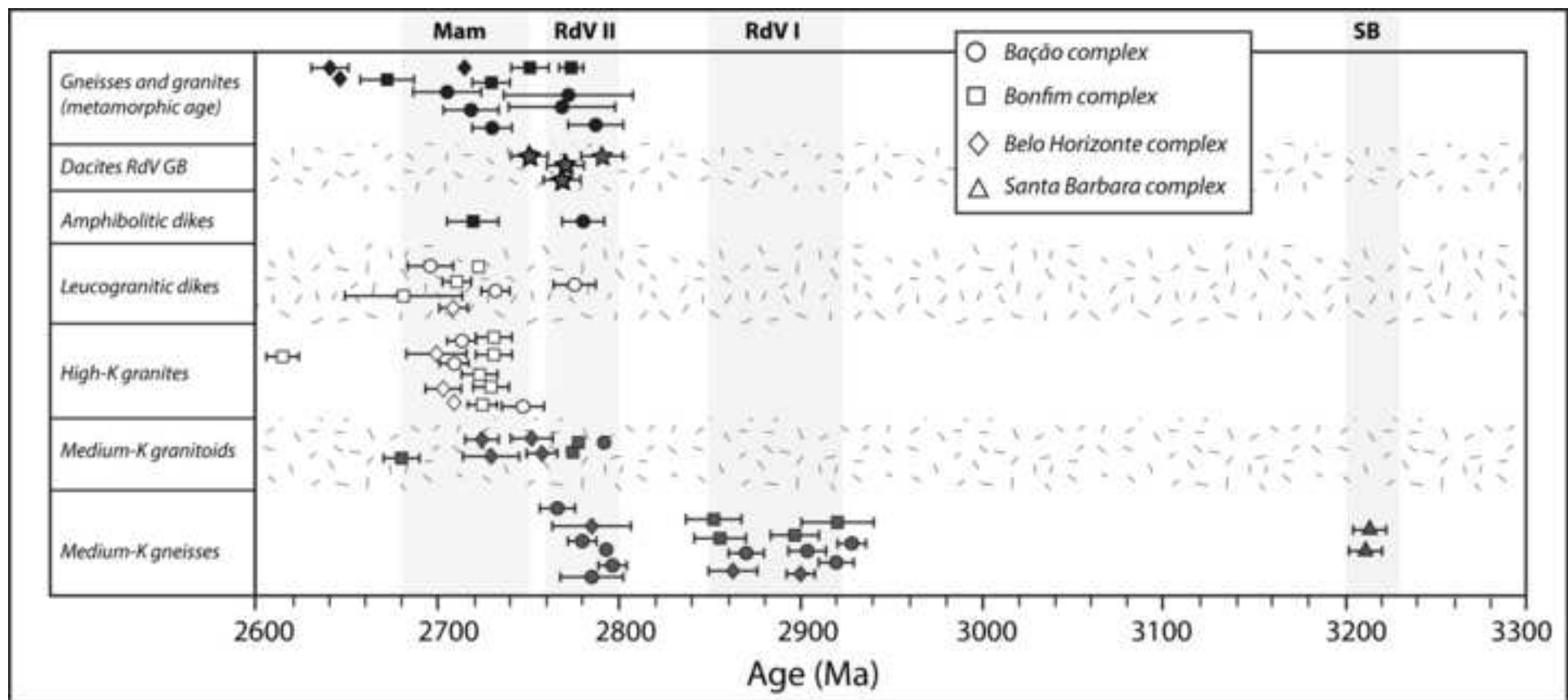




Figure 9  
[Click here to download high resolution image](#)



Figure 10

[Click here to download high resolution image](#)

## Rio das Velhas Sg. - Nova Lima Gr.

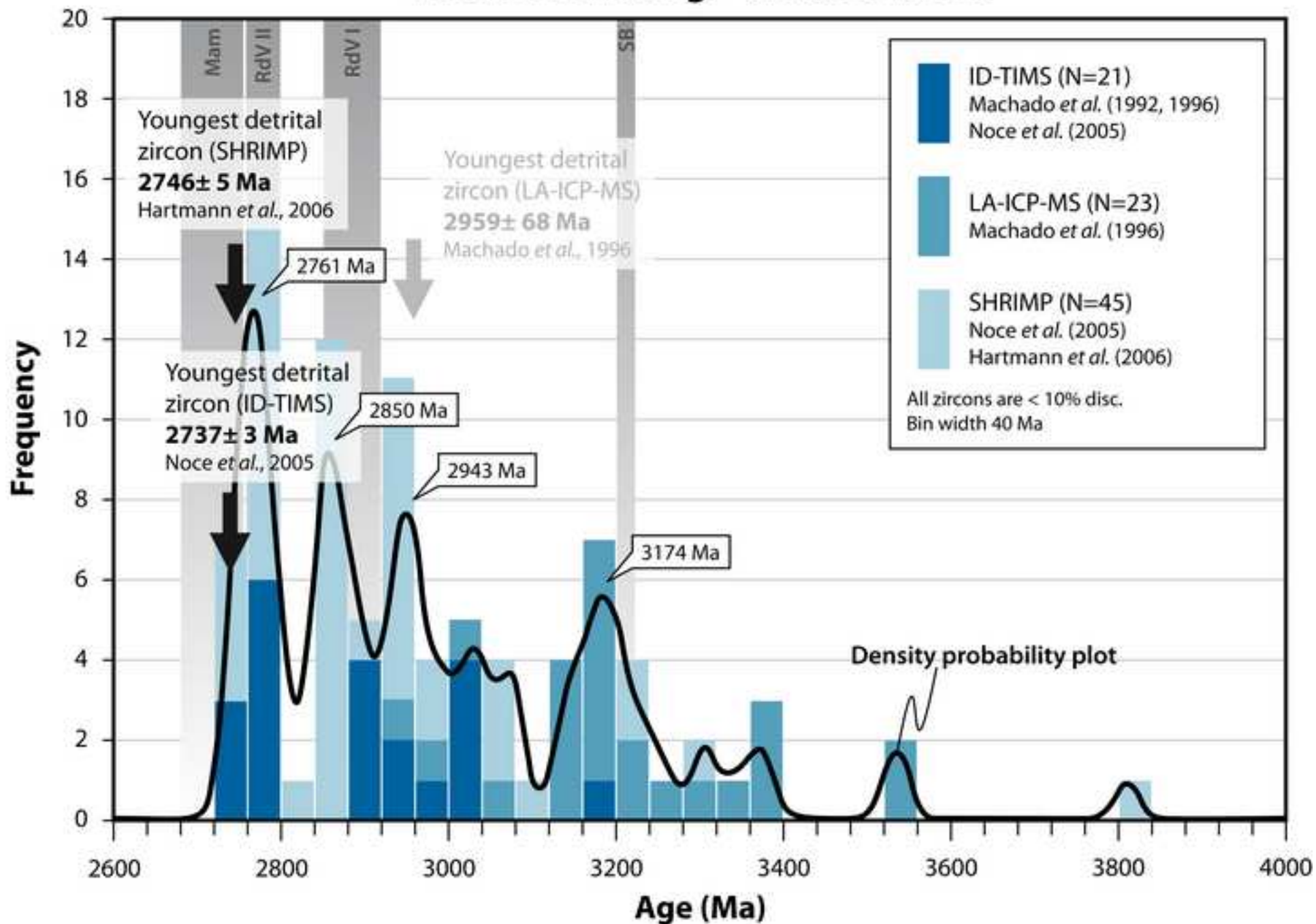




Figure 11

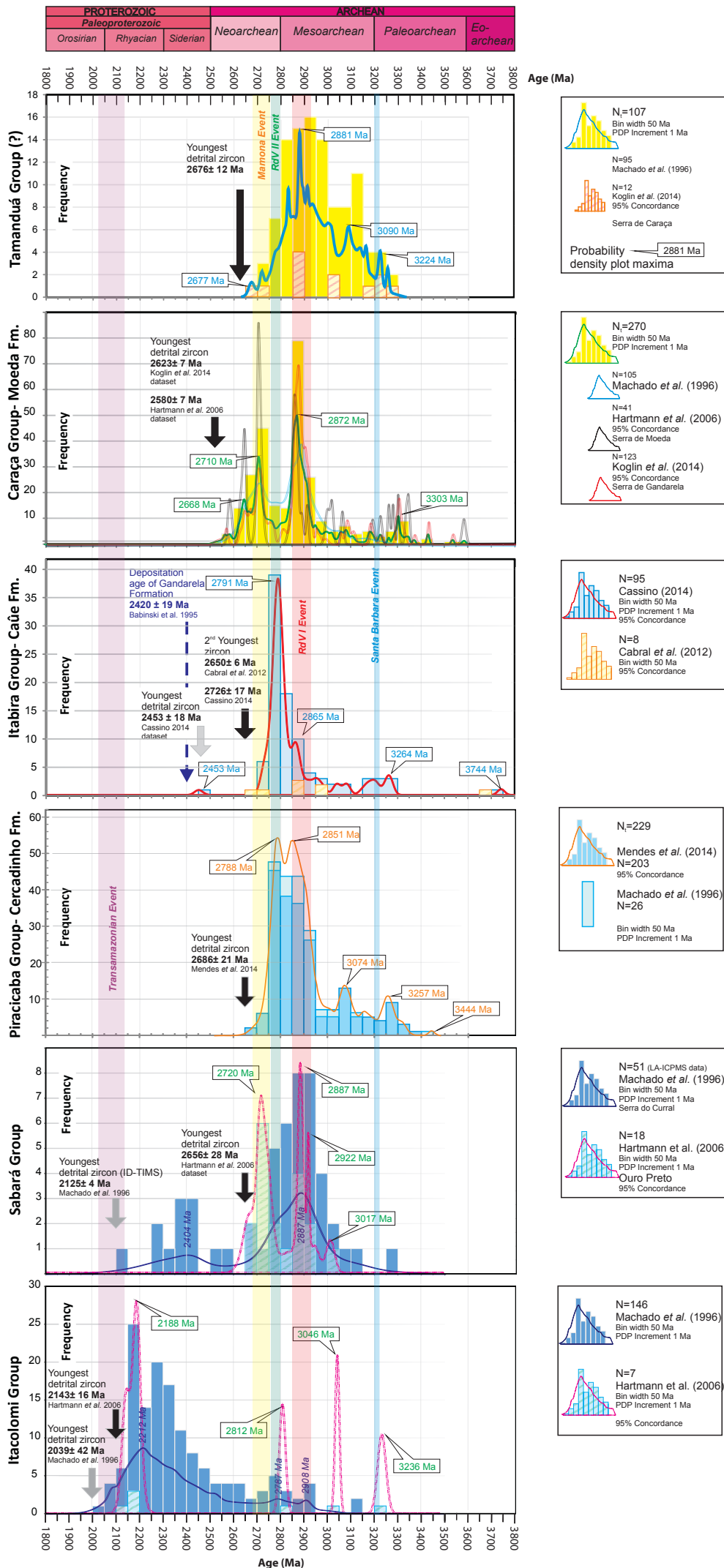


Figure 12  
[Click here to download high resolution image](#)

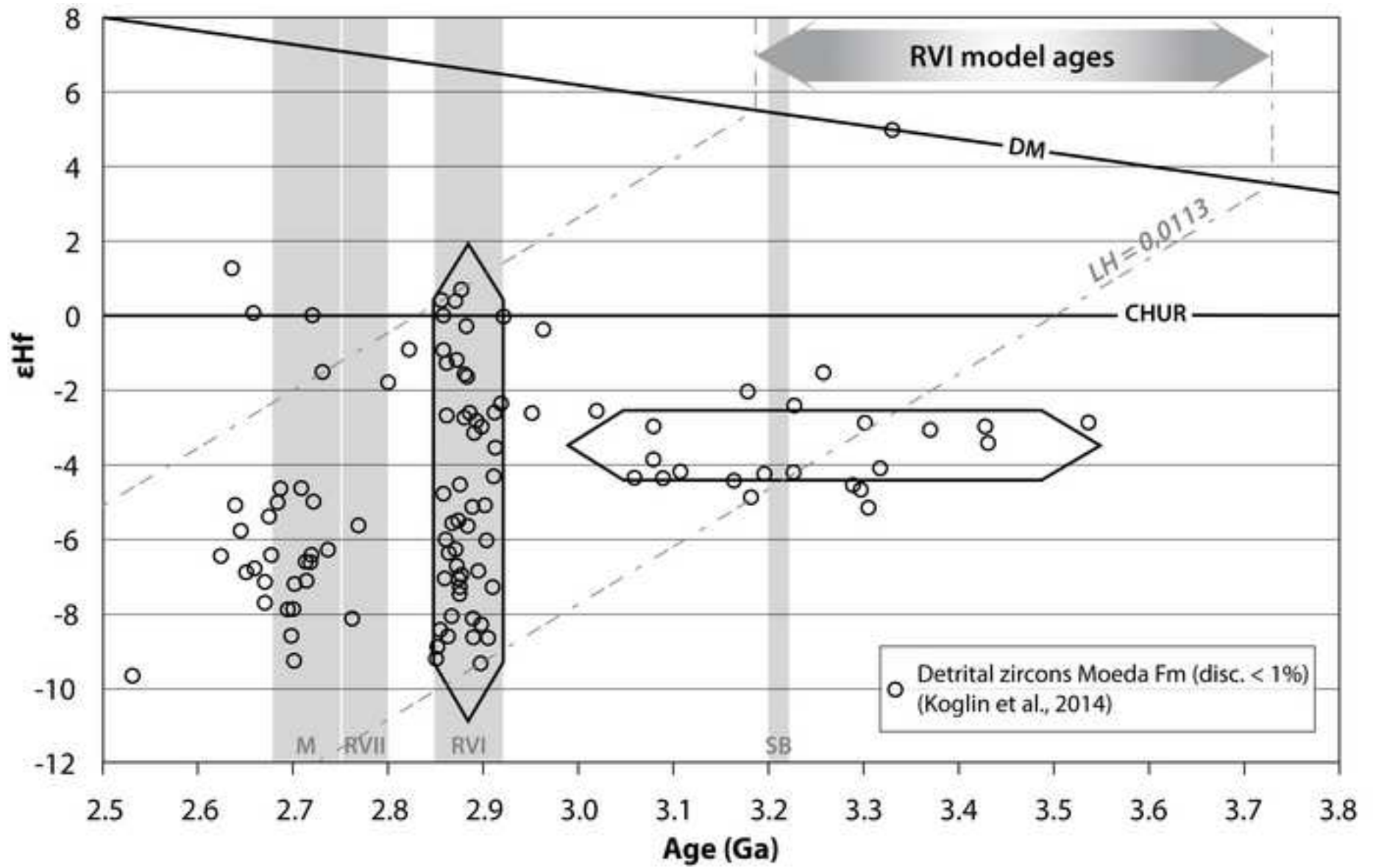
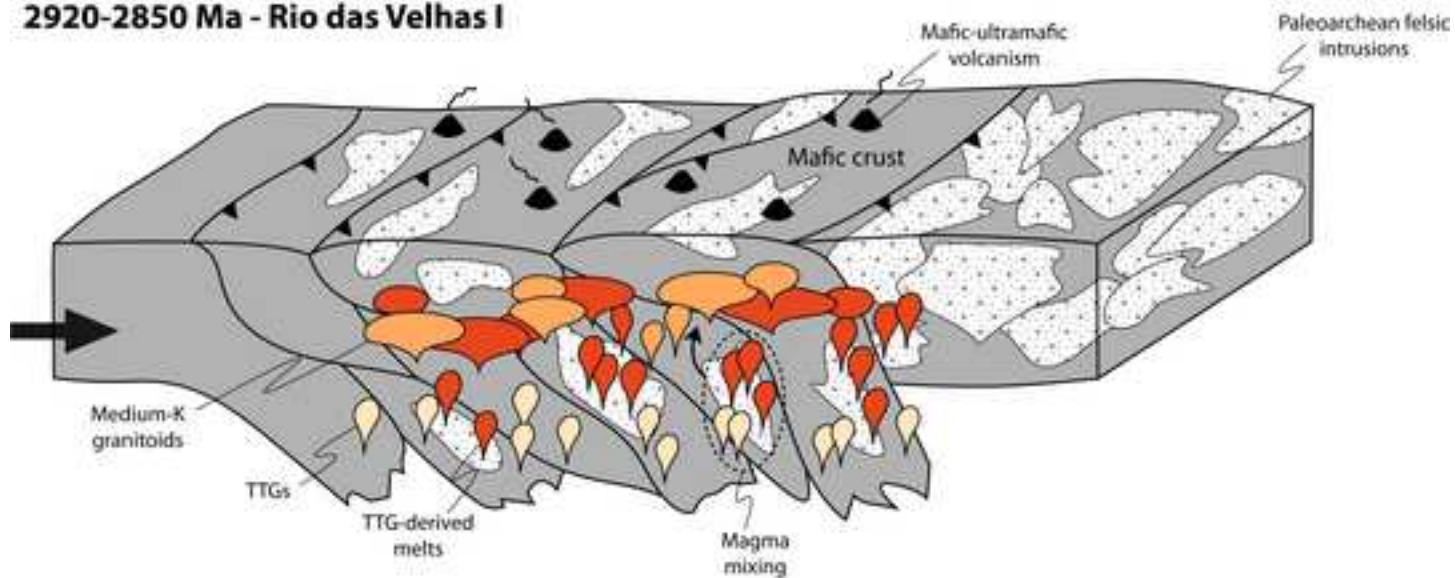




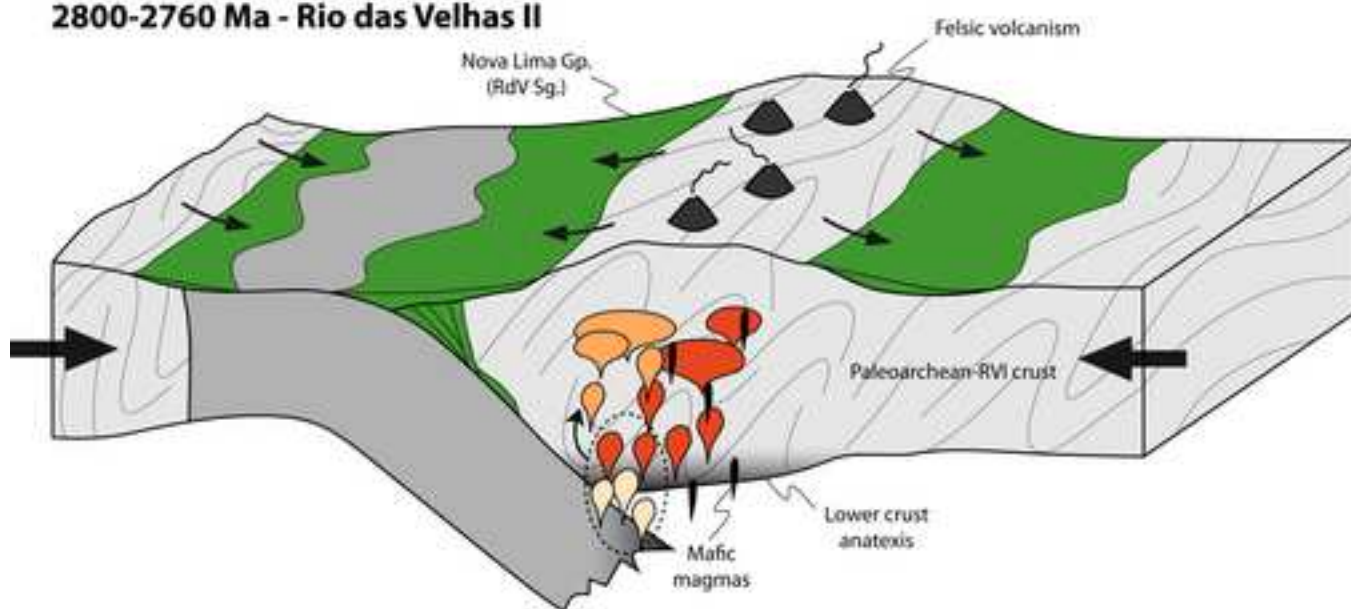
Figure 13

[Click here to download high resolution image](#)

### 2920-2850 Ma - Rio das Velhas I



### 2800-2760 Ma - Rio das Velhas II



### 2760-2680 Ma - Mamona

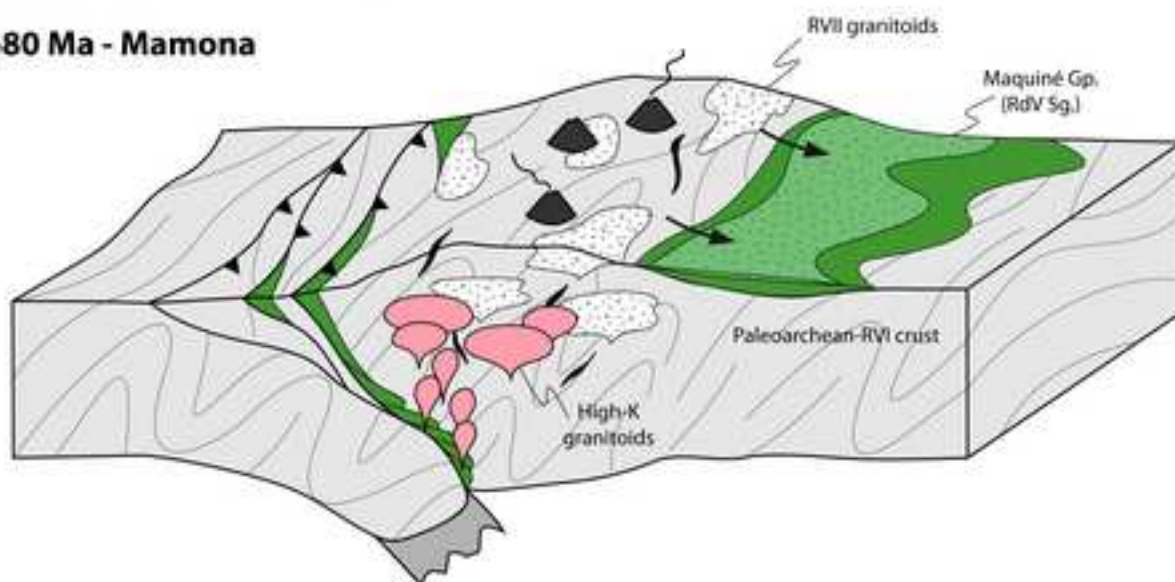


Table A: Major and trace element composition of igneous rocks from the Quadrilátero Ferrífero

Sample	FQ1	FQ2	FQ3	FQ4	FQ5	FQ6	FQ7	FQ8	FQ10
Dome/Group	Baç	Baç	Baç	Baç	Baç	Baç	Baç	Baç	Baç
Field group	Granite	Gneiss	Leucogr.	Gneiss	Granite	Gneiss	Granite	Gneiss	Gneiss
Reference	1	1	1	1	1	1	1	1	1
SiO <sub>2</sub>	74.41	72.44	71.09	73.41	74.31	70.79	75.29	73.56	72.59
TiO <sub>2</sub>	0.21	0.50	0.04	0.22	0.17	0.49	0.08	0.36	0.31
Al <sub>2</sub> O <sub>3</sub>	13.90	14.43	16.00	14.93	14.32	14.99	13.66	13.90	14.97
Fe <sub>2</sub> O <sub>3</sub> tot	1.51	2.75	0.42	1.54	1.59	3.14	0.90	2.23	2.01
MnO	0.01	0.03	0.03	0.03	0.02	0.03	0.01	0.05	0.03
MgO	0.21	1.01	0.04	0.44	0.30	0.78	0.15	0.47	0.64
CaO	0.92	2.14	0.36	1.84	1.44	2.45	0.90	1.03	2.38
Na <sub>2</sub> O	3.00	4.49	3.03	4.63	4.27	3.58	3.30	3.56	5.02
K <sub>2</sub> O	5.74	2.09	8.93	2.89	3.54	3.61	5.67	4.73	1.95
P <sub>2</sub> O <sub>5</sub>	0.08	0.13	0.04	0.07	0.04	0.15	0.03	0.11	0.09
LOI	0.6	0.9	0.32	0.85	0.75	1.05	0.42	0.69	0.67
K <sub>2</sub> O/Na <sub>2</sub> O	1.92	0.46	2.94	0.62	0.83	1.01	1.72	1.33	0.39
Sc	5.1	9.2	4.4	5.8	5.8	7.0	3.9	7.0	4.4
V	16.0	51.8	13.0	24.6	16.1	38.8	12.4	25.8	26.5
Cr	8.8	8.5	8.0	10.4	14.3	23.2	10.6	21.4	18.6
Co	81.3	53.1	60.6	71.8	88.9	57.9	76.6	48.2	59.2
Ni	4.5	6.1	5.0	7.2	7.7	9.7	4.8	7.6	9.0
Cu	8.2	15.2	5.1	10.7	14.7	36.2	5.8	5.9	11.3
Zn	44.0	56.3	14.6	64.4	45.3	67.7	33.7	63.1	55.3
Rb	211	63	267	93	100	152	212	343	76
Sr	70	240	98	375	126	154	60	59	414
Y	7.8	42.3	4.7	7.8	22.6	24.5	39.7	58.7	8.8
Zr	112	216	13	127	127	311	86	178	156
Nb	10.9	15.0	6.2	5.5	18.9	21.1	11.4	24.7	6.3
Mo	0.7	0.3	0.3	0.4	0.6	1.6	0.5	0.9	0.3
Cs	9.5	4.4	7.3	3.9	2.7	6.2	15.2	17.3	6.7
Ba	442	596	418	696	776	940	424	296	537
La	24.02	24.41	2.87	14.11	38.90	66.77	19.33	42.32	35.03
Ce	55.14	49.73	4.65	33.86	78.85	152.24	43.44	93.58	59.75
Pr	6.50	5.90	0.39	2.79	8.28	14.56	4.58	10.96	6.00
Nd	22.69	24.17	1.22	9.76	29.04	52.01	16.04	42.56	20.06
Sm	4.49	5.84	0.38	1.87	6.03	8.39	4.29	10.04	3.30
Eu	0.60	1.38	0.37	0.58	1.08	1.55	0.61	0.43	0.82
Gd	2.58	6.69	0.42	1.66	5.12	5.97	5.03	10.21	2.57
Tb	0.35	1.12	0.09	0.29	0.79	0.85	0.99	1.76	0.34
Dy	1.54	7.57	0.69	1.50	4.52	4.66	6.72	10.63	1.69
Ho	0.27	1.54	0.16	0.31	0.94	0.87	1.44	2.13	0.32
Er	0.72	4.66	0.67	0.74	2.29	2.48	4.07	6.05	0.86
Tm	0.11	0.71	0.13	0.13	0.36	0.33	0.62	0.92	0.13
Yb	0.77	4.66	1.01	0.81	2.32	2.19	3.84	6.23	0.79
Lu	0.13	0.74	0.17	0.12	0.32	0.35	0.52	0.87	0.12
Hf	3.49	6.35	0.57	3.69	4.28	8.38	3.85	5.78	4.44
Ta	1.52	1.73	2.28	1.05	1.54	1.55	1.76	3.04	1.44
Pb	48.9	12.4	47.1	29.3	35.3	31.8	66.1	35.0	21.0
Th	15.5	7.5	1.0	5.9	18.2	20.3	15.2	35.9	9.6
U	3.3	2.1	3.0	1.5	2.8	2.7	3.9	11.1	2.6

Abbreviations: Baç - Bação complex; Bo- Bonfim complex; Ca- Caeté complex; BH- Belo Horizonte complex; RdV- Rio das Velhas greenstone